present study, was included in this network. On the other hand, the gene network for down-regulated genes included those linked to the heat-shock protein response, such as HSPA1A, HSPA2, HSPA4L, HSPA8, HSPA12A, and HSPH1 (Fig. 3B).

3.3. GDF15 as a potential biomarker for diagnosis and evaluating the therapeutic efficacy of pyruvate

Proteins encoded by genes related to intracellular energy deficiency in 2SD cells and secreted into the medium could be potential biomarkers for mitochondrial diseases. Gene annotation analysis revealed the location of gene products that were specifically up- and down-regulated by lactate at 8 h (231 and 75 genes, respectively) (Table 1). Twenty-three up-regulated genes and 4 down-regulated genes were annotated to the extracellular space, each of which is listed in Tables 2 and 3. Among them, we focused on the top 2 ranked up-regulated genes, growth differentiation factor 15 (GDF15) and inhibin beta E (INHBE).

To validate the intracellular expression levels of these genes, we performed quantitative RT-PCR for GDF15 and INHBE. The expression levels of GDF15 (Fig. 4A) and INHBE (Fig. 4B) in the 2SD cells were increased by treatment with 10 mM lactate, but not with 10 mM pyruvate, for 4 or 8 h. Furthermore, GDF15 expression at 0 h was higher in 2SD cells than in 2SA cells. These results confirmed the reproducibility of our microarray data and identified GDF15 and INHBE as candidate biomarkers. To determine whether the secretion of GDF15 and INHBE proteins was increased in 2SD cells in response to lactate treatment, we measured their concentrations in medium from 2SA and 2SD cells cultured for 24 h in the presence of 1 mM pyruvate, 10 mM lactate, or 10 mM pyruvate. ELISA showed that the GDF15 levels were higher in the conditioned medium of 2SD cells than in that of 2SA cells under all of the culture conditions (Fig. 4C). Moreover, treatment with 10 mM lactate, but not with 10 mM pyruvate, promoted secretion of GDF15 in 2SD cells in comparison with treatment with 1 mM pyruvate, whereas 2SA cells did not respond to the high dose of lactate and pyruvate treatment. In contrast, INHBE protein was not detectable by ELISA in the conditioned medium of either 2SD or 2SA cells under any culture conditions (data not shown). These results indicate that GDF15 could be a potential biomarker for diagnosis and monitoring the disease status and progression as well as for assessing the therapeutic efficacy of pyruvate for the treatment of mitochondrial diseases.

3.4. GDF15 as a biomarker for diagnosis of mitochondrial diseases

In order to validate the feasibility of GDF15 as a serum biomarker, we measured its concentration in the serum of 17 patients with mitochondrial diseases as well as in that of 13 patients with other pediatric diseases as a control (Supplementary Table 2). ELISA showed that the average concentration of GDF15 in the serum of mitochondrial disease patients was 2632.9 pg/mL, whereas that for other pediatric disease patients was 285.2 pg/mL, suggesting that GDF15 levels were significantly increased in the serum of mitochondrial disease patients and could clearly distinguish mitochondrial disease patients from control patients (Fig. 5A).

Table 1
The location of probes (genes) up- and down-regulated in 2SD cells with lactate treatment for 8 h.

Location	Up-regulated		Down-regulated	
	Probe number	Gene number	Probe number	Gene number
Nucleus	39	35	14	14
Cytoplasm	51	47	25	19
Plasma membrane	37	33	16	16
Extracellular space	26	23	5	4
Unknown	160	93	36	22

Since fibroblast growth factor 21 (FGF21) was recently proposed as a diagnostic marker for mitochondrial diseases (Davis et al., 2013; Suomalainen et al., 2011), we also measured the FGF21 levels in the serum of the same mitochondrial disease patients and control patients (Fig. 5B). The serum FGF21 levels were higher in patients with mitochondrial diseases than in those with other diseases. Furthermore, there was a good correlation between the serum GDF15 and FGF21 levels (Fig. 5C).

In an attempt to find additional biomarkers, we determined the serum levels of 21 cytokines in the same patients by using the multiplex suspension array. As shown in Supplementary Fig. 4A, the serum concentrations of HGF and SCF were higher in patients with mitochondrial diseases than in control patients, whereas the serum levels of SCGF-β were lower in the former than in the latter.

Finally, we performed ROC curve analysis of GDF15, HGF, SCF, SCGF-β, and FGF21. As shown in Fig. 5D, the area under the curves (AUC) for GDF15 (0.986) was higher than that for FGF21 (0.787). The AUC for FGF21 was similar to those for HGF (0.747), SCF (0.729), and SCGF-β (0.837) (Supplementary Fig. 4B), indicating that GDF15 had the maximum sensitivity and specificity for diagnosis of mitochondrial diseases. These results suggest that GDF15 has the greatest potential as a novel diagnostic marker for MELAS and other mitochondrial diseases.

4. Discussion

Based on the global gene expression analysis of cybrid cells with mitochondrial dysfunction, we identified GDF15 as a potential biomarker whose expression and secretion reflected the intracellular energy deficiency and the effect of pyruvate therapy on the energy metabolism. We then determined the serum levels of GDF15 in patients with mitochondrial diseases and other diseases and identified GDF15 as a novel diagnostic marker for mitochondrial diseases. Although additional clinical studies are needed, the serum GDF15 concentration may be a useful biomarker not only for diagnosis of mitochondrial diseases but also for monitoring the disease status and progression as well as for determining the efficacy of pyruvate therapy.

GDF15 is a member of the transforming growth factor-β (TGF-β) superfamily and is widely expressed in mammalian tissues (Unsicker et al., 2013). GDF15 plays important roles in multiple pathologies including cardiovascular diseases, cancer, and inflammation. It has been shown that GDF15 is up-regulated by tumor suppressor p53 in response to high glucose or treatment with anti-cancer compounds (Baek et al., 2002; Li et al., 2013; Yang et al., 2003). The p53 protein is a transcription factor that responds to a variety of stresses such as DNA damage, oxidative stress, hypoxia, and metabolic stress, and it activates the expression of genes to induce cell cycle arrest, DNA repair, senescence, and cell death (Sermeus and Michiels, 2011; Sperka et al., 2012; Zhang et al., 2010). CDKN1A (p21), a potent cyclin-dependent kinase inhibitor, is a major downstream effector of p53, which induces cell-cycle arrest (Sperka et al., 2012). In our microarray data, the CDKN1A expression level was 3.5-fold increased by lactate treatment of 2SD cells (data not shown). Previous reports demonstrated increased expression of CDKN1A in the skeletal muscle of patients with mitochondrial diseases and a cell line depleted of mitochondrial DNA (Behan et al., 2005; Crimi et al., 2005). Besides CDKN1A, we found other p53 effector genes in the list of genes up-regulated in the lactate-treated 2SD cells, including GADD45A, EGR2, DDIT3, CHMP4C, SESN2, ULBP1, DDIT4, and NUPR1 (data not shown). These results suggest that p53 activation may have played an important role in the induction of GDF15 expression in 2SD cells treated with lactate. It has been also demonstrated that p53 activation caused by metabolic stress is mediated by AMP-activated protein kinase (AMPK; Zhang et al., 2010). Our previous metabolomic profiling revealed that the ATP level drops but that the ADP and AMP levels are increased in lactate-treated 2SD cells (Kami et al., 2012), implying that elevation of the AMP/ATP ratio may activate p53 through AMPK activation. Taken together, it is possible that p53 induced GDF15 expression in

Table 2
Genes annotated to the extracellular space among those specifically up-regulated by lactate treatment for 8 h.

Gene symbol	Accession number	Entrez gene name	Fold change	
			L-8/L-0[a]	L-8/P-8[b]
GDF15	NM_004864	Growth differentiation factor 15	27.4	14.8
INHBE	NM_031479	Inhibin, beta E	15.0	9.4
AREG	NM_001657	Amphiregulin	14.0	2.2
ECM2	NM_001393	Extracellular matrix protein 2, female organ and adipocyte specific	11.8	9.0
ADM2	NM_024866	Adrenomedullin 2	10.3	3.0
MMP3	NM_002422	Matrix metallopeptidase 3 (stromelysin 1, progelatinase)	9.8	4.2
IL1A	NM_000575	Interleukin 1, alpha	7.6	6.0
C12orf39	ENST00000256969	Chromosome 12 open reading frame 39	6.3	6.7
APOL6	NM_030641	Apolipoprotein L, 6	6.2	3.8
SCG5	NM_003020	Secretogranin V (7B2 protein)	5.2	3.0
SPOCK2	NM_014767	Sparc/osteonectin, cwcv and kazal-like domains proteoglycan (testican) 2	5.1	6.6
AMTN	NM_212557	Amelotin	5.0	3.9
IL23A	NM_016584	Interleukin 23, alpha subunit p19	4.4	2.8
ADAMTS17	NM_139057	ADAM metallopeptidase with thrombospondin type 1 motif, 17	3.5	2.2
VEGFA	NM_001025370	Vascular endothelial growth factor A	3.4	2.5
STC2	NM_003714	Stanniocalcin 2	3.4	2.6
PDGFB	NM_002608	Platelet-derived growth factor beta polypeptide	2.8	3.8
C1QTNF1	NM_198594	C1q and tumor necrosis factor related protein 1	2.6	2.9
HECW2	NM_020760	HECT, C2 and WW domain containing E3 ubiquitin protein ligase 2	2.4	2.1
IGFALS	NM_004970	Insulin-like growth factor binding protein, acid labile subunit	2.3	2.5
IGFBP1	NM_000596	Insulin-like growth factor binding protein 1	2.3	2.1
PDGFA	NM_002607	Platelet-derived growth factor alpha polypeptide	2.2	2.2
CLEC3B	NM_003278	C-type lectin domain family 3, member B	2.1	2.2

[a]Fold change between 8 h and 0 h after lactate treatment
[b]Fold change between lactate treatment and pyruvate treatment at 8 h

response to AMPK activation caused by the intracellular energy deficiency. However, it remains to be determined whether other stresses such as oxidative stress may also have participated in p53 activation and GDF15 induction in the lactate-treated 2SD cells.

Gene network analysis demonstrated that the top-ranked network contained not only genes associated with the amino-acid starvation response but also the GDF15 gene (Fig. 3A). In a mouse model of late-onset mitochondrial myopathy, the expression of amino-acid starvation-responsive genes was shown to be elevated (Tyynismaa et al., 2010). The asparagine synthetase (ASNS), which is a representative gene involved in the amino-acid starvation response, has been reported to be up-regulated in the skeletal muscle of patients with mitochondrial diseases and in cybrid cells established from a mitochondrial disease patient (Crimi et al., 2005; Fujita et al., 2007). Activating transcription factor 4 (ATF4) is a master regulator of integrated stress responses (ISR), in which a variety of stresses, including amino-acid starvation as well as glucose starvation, ER stress, hypoxia, and oxidative stress, induce phosphorylation of eIF2α followed by up-regulation of ATF4 to activate expression of stress-responsive genes (Harding et al., 2003; Jiang et al., 2004; Rouschop et al., 2010; Rzymski et al., 2010; Teske et al., 2011). It is noteworthy to point out that GDF15 has been shown to be up-regulated by ATF4 in mouse embryonic fibroblasts (Jousse et al., 2007). Taken together, such findings suggest that the ISR pathway may also contribute to the induction of GDF15 in response to defective energy metabolism and play a role in the pathogenesis of mitochondrial diseases.

In the present study, we validated the clinical usefulness of GDF15 as a diagnostic marker by determining the serum GDF15 levels in patients with mitochondrial diseases and in those with other pediatric diseases. The results showed that serum GDF15 levels were significantly elevated in patients with mitochondrial diseases, which finding is consistent with a recent report (Kalko et al., 2014). We also demonstrated that GDF15 had higher sensitivity and specificity than FGF21, which was recently identified as a sensitive and specific blood biomarker for muscle pathology in a wide range of mitochondrial diseases in adults and children (Suomalainen et al., 2011). Our small-scale study, however, may have underestimated the clinical usefulness of FGF21, because the AUC for FGF21 reported by 2 independent groups (0.95 and 0.91) was higher than that in the present study (0.787).

Using the multiplex suspension array, we also identified HGF, SCF, and SCGF-β as potential diagnostic markers for mitochondrial diseases. The ROC curve analysis, however, revealed that GDF15 had the maximum sensitivity and specificity for diagnosis of mitochondrial diseases compared with HGF, SCF, SCGF-β, or FGF21. Based on the microarray analysis, we also selected INHBE as the next best candidate gene (Table 2). INHBE is a member of the activin beta family, which has been reported to be primarily expressed in the liver and up-regulated by drug-induced ER stress, cysteine deprivation, and insulin treatment (Bruning et al., 2012; Dombroski et al., 2010; Hashimoto et al., 2009; Lee et al., 2008). Although secreted INHBE protein was not detectable in the conditioned medium from the cell cultures, we are currently investigating the clinical usefulness of INHBE as a biomarker for diagnosis and monitoring of the disease status and progression.

Table 3
Genes annotated to the extracellular space among those specifically down-regulated by lactate treatment for 8 h.

Gene symbol	Accession number	Entrez gene name	Fold change	
			L-8/L-0[a]	L-8/P-8[b]
CXCL1	NM_001511	Chemokine (C-X-C motif) ligand 1 (melanoma growth stimulating activity, alpha)	−3.4	−2.6
PDZRN3	NM_015009	PDZ domain containing ring finger 3	−2.4	−2.0
SLC39A10	NM_020342	Solute carrier family 39 (zinc transporter), member 10	−2.3	−2.9
DKK1	NM_012242	Dickkopf 1 homolog (Xenopus laevis)	−2.1	−2.3

[a]Fold change between 8 h and 0 h after lactate treatment
[b]Fold change between lactate treatment and pyruvate treatment at 8 h

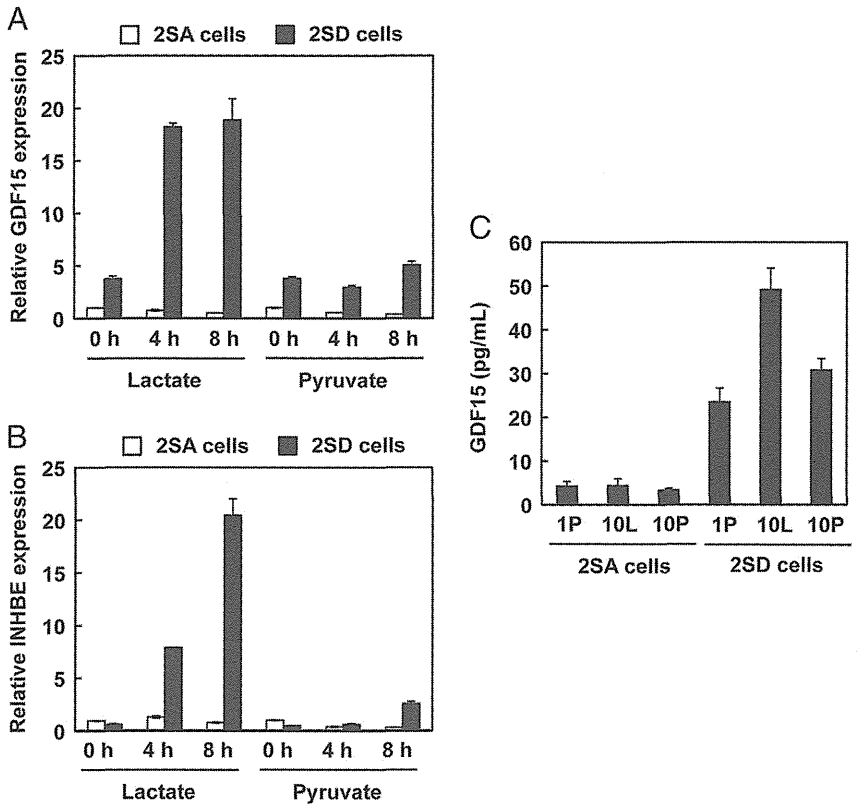

Fig. 4. Quantitative RT-PCR and ELISA for GDF15 and INHBE Total RNA isolated from 2SA and 2SD cells treated with 10 mM lactate or 10 mM pyruvate for 0, 4 or 8 h (n = 3) were subjected to quantitative RT-PCR for GDF15 (A) and INHBE (B). (C) The conditioned medium collected from 2SA and 2SD cell cultures treated with 10 mM lactate (10 L), 10 mM pyruvate (10P) or 1 mM pyruvate (1P) for 24 h was subjected to ELISA for GDF15 protein ($n = 3$).

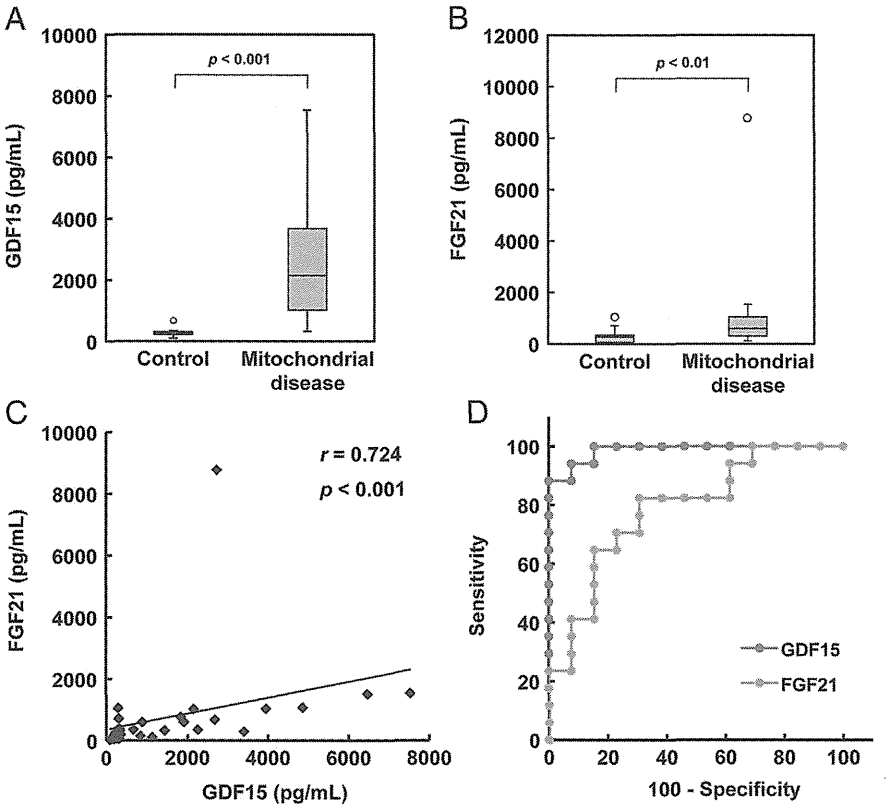

Fig. 5. Measurement of the GDF15 and FGF21 concentrations in the serum of patients. The serum GDF15 (A) and FGF21 (B) concentrations in 17 patients with mitochondrial diseases as well as those in 13 patients with other pediatric diseases were determined by ELISA. The outlier is shown with an open symbol. (C) A correlation analysis between the serum GDF15 and FGF21 levels was performed for the patients described above by use of IBM SPSS statistics. (D) The ROC curve analysis for GDF15 and FGF21 was performed. Areas under the curves (AUC) for GDF15 and FGF21 were 0.986 (95% CI 0.957-1.000) and 0.787 (95% CI 0.621-0.953), respectively.

It is well known that mitochondrial dysfunction is associated with the pathology of various diseases such as Parkinson's disease, Alzheimer's disease, diabetes, and aging (Exner et al., 2012; Lopez-Otin et al., 2013; Martin and McGee, 2014). GDF15, which may reflect mitochondria dysfunction, could be a useful marker for those diseases and the aging process. In support of this idea, the serum GDF15 level was reported to be elevated under various pathological conditions such as cancers, cardiovascular diseases, diabetes, and obesity (Dostalova et al., 2009; Kempf et al., 2007; Welsh et al., 2003); however, in most cases, it was not as high as that observed in mitochondrial diseases. Recent cohort studies also demonstrated that the serum GDF15 level is a novel predictor of all-cause mortality and is associated with cognitive performance and cognitive decline (Fuchs et al., 2013; Wiklund et al., 2010). We thus anticipate that GDF15 will attract more interest with respect to a variety of diseases and aging associated with mitochondrial dysfunction.

In conclusion, we identified GDF15 as a novel serum marker for the diagnosis of mitochondrial diseases and possibly both for monitoring the disease status and progression and for evaluating the therapeutic efficacy of pyruvate. Large-scale clinical trials including combined use of other markers such as FGF21 should confirm the clinical usefulness of GDF15.

Acknowledgments

This study was supported in part by the Ministry of Education, Culture, Sports, Science, and Technology of Japan; GMEXT/JSPS KAKENHI Grant Number: A-25242062, A-22240072, B-21390459, C-26670481, C-21590411, CER-24650414 (to M.T.), C-26350922 (to Y.F.), C-25461571 (to Y.K.), and YSB-25860891 (to S.Y.); the Ministry of Health, Labor, and Welfare of Japan; Grants-in-Aid for Research on Intractable Diseases (Mitochondrial Disorders): 23-Nanchi-Ippan-016, 23-Nanchi-Ippan-116, and 24-Nanchi-Ippan-005 (to M.T., and Y.K.); and the Takeda Science Foundation (to M.T.).

Appendix A. Supplementary data

Supplementary data to this article can be found online at http://dx.doi.org/10.1016/j.mito.2014.10.006.

References

Baek, S.J., Wilson, L.C., Eling, T.E., 2002. Resveratrol enhances the expression of non-steroidal anti-inflammatory drug-activated gene (NAG-1) by increasing the expression of p53. Carcinogenesis 23, 425–434.

Behan, A., Doyle, S., Farrell, M., 2005. Adaptive responses to mitochondrial dysfunction in the rho degrees Namalwa cell. Mitochondrion 5, 173–193.

Bruning, A., Matsingou, C., Brem, G.J., Rahmeh, M., Mylonas, I., 2012. Inhibin beta E is upregulated by drug-induced endoplasmic reticulum stress as a transcriptional target gene of ATF4. Toxicol. Appl. Pharmacol. 264, 300–304.

Chomyn, A., Martinuzzi, A., Yoneda, M., Daga, A., Hurko, O., Johns, D., Lai, S.T., Nonaka, I., Angelini, C., Attardi, G., 1992. MELAS mutation in mtDNA binding site for transcription termination factor causes defects in protein synthesis and in respiration but no change in levels of upstream and downstream mature transcripts. Proc. Natl. Acad. Sci. U. S. A. 89, 4221–4225.

Crimi, M., Bordoni, A., Menozzi, G., Riva, L., Fortunato, F., Galbiati, S., Del Bo, R., Pozzoli, U., Bresolin, N., Comi, G.P., 2005. Skeletal muscle gene expression profiling in mitochondrial disorders. Faseb J. 19, 866–868.

Davis, R.L., Liang, C., Edema-Hildebrand, F., Riley, C., Needham, M., Sue, C.M., 2013. Fibroblast growth factor 21 is a sensitive biomarker of mitochondrial disease. Neurology 81, 1819–1826.

Dombroski, B.A., Nayak, R.R., Ewens, K.G., Ankener, W., Cheung, V.G., Spielman, R.S., 2010. Gene expression and genetic variation in response to endoplasmic reticulum stress in human cells. Am. J. Hum. Genet. 86, 719–729.

Dostalova, I., Roubicek, T., Bartlova, M., Mraz, M., Lacinova, Z., Haluzikova, D., Kavalkova, P., Matoulek, M., Kasalicky, M., Haluzik, M., 2009. Increased serum concentrations of macrophage inhibitory cytokine-1 in patients with obesity and type 2 diabetes mellitus: the influence of very low calorie diet. Eur. J. Endocrinol. 161, 397–404.

Exner, N., Lutz, A.K., Haass, C., Winklhofer, K.F., 2012. Mitochondrial dysfunction in Parkinson's disease: molecular mechanisms and pathophysiological consequences. EMBO J. 31, 3038–3062.

Fuchs, T., Trollor, J.N., Crawford, J., Brown, D.A., Baune, B.T., Samaras, K., Campbell, L., Breit, S.N., Brodaty, H., Sachdev, P., Smith, E., 2013. Macrophage inhibitory cytokine-1 is associated with cognitive impairment and predicts cognitive decline - the Sydney Memory and Aging Study. Aging Cell 12, 882–889.

Fujita, Y., Ito, M., Nozawa, Y., Yoneda, M., Oshida, Y., Tanaka, M., 2007. CHOP (C/EBP homologous protein) and ASNS (asparagine synthetase) induction in cybrid cells harboring MELAS and NARP mitochondrial DNA mutations. Mitochondrion 7, 80–88.

Goto, Y., Nonaka, I., Horai, S., 1990. A mutation in the tRNA(Leu)(UUR) gene associated with the MELAS subgroup of mitochondrial encephalomyopathies. Nature 348, 651–653.

Goto, Y., Horai, S., Matsuoka, T., Koga, Y., Nihei, K., Kobayashi, M., Nonaka, I., 1992. Mitochondrial myopathy, encephalopathy, lactic acidosis, and stroke-like episodes (MELAS): a correlative study of the clinical features and mitochondrial DNA mutation. Neurology 42, 545–550.

Harding, H.P., Zhang, Y., Zeng, H., Novoa, I., Lu, P.D., Calfon, M., Sadri, N., Yun, C., Popko, B., Paules, R., Stojdl, D.F., Bell, J.C., Hettmann, T., Leiden, J.M., Ron, D., 2003. An integrated stress response regulates amino acid metabolism and resistance to oxidative stress. Mol. Cell 11, 619–633.

Hashimoto, O., Sekiyama, K., Matsuo, T., Hasegawa, Y., 2009. Implication of activin E in glucose metabolism: transcriptional regulation of the inhibin/activin betaE subunit gene in the liver. Life Sci. 85, 534–540.

Jiang, H.Y., Wek, S.A., McGrath, B.C., Lu, D., Hai, T., Harding, H.P., Wang, X., Ron, D., Cavener, D.R., Wek, R.C., 2004. Activating transcription factor 3 is integral to the eukaryotic initiation factor 2 kinase stress response. Mol. Cell. Biol. 24, 1365–1377.

Jousse, C., Deval, C., Maurin, A.C., Parry, L., Cherasse, Y., Chaveroux, C., Lefloch, R., Lenormand, P., Bruhat, A., Fafournoux, P., 2007. TRB3 inhibits the transcriptional activation of stress-regulated genes by a negative feedback on the ATF4 pathway. J. Biol. Chem. 282, 15851–15861.

Kalko, S.G., Paco, S., Jou, C., Rodriguez, M.A., Meznaric, M., Rogac, M., Jekovec-Vrhovsek, M., Sciacco, M., Moggio, M., Fagiolari, G., De Paepe, B., De Meirleir, L., Ferrer, I., Roig-Quilis, M., Munell, F., Montoya, J., Lopez-Gallardo, E., Ruiz-Pesini, E., Artuch, R., Montero, R., Torner, F., Nascimento, A., Ortez, C., Colomer, J., Jimenez-Mallebrera, C., 2014. Transcriptomic profiling of TK2 deficient human skeletal muscle suggests a role for the p53 signalling pathway and identifies growth and differentiation factor-15 as a potential novel biomarker for mitochondrial myopathies. BMC Genomics 15, 91.

Kami, K., Fujita, Y., Igarashi, S., Koike, S., Sugawara, S., Ikeda, S., Sato, N., Ito, M., Tanaka, M., Tomita, M., Soga, T., 2012. Metabolomic profiling rationalized pyruvate efficacy in cybrid cells harboring MELAS mitochondrial DNA mutations. Mitochondrion 12, 644–653.

Kempf, T., Horn-Wichmann, R., Brabant, G., Peter, T., Allhoff, T., Klein, G., Drexler, H., Johnston, N., Wallentin, L., Wollert, K.C., 2007. Circulating concentrations of growth-differentiation factor 15 in apparently healthy elderly individuals and patients with chronic heart failure as assessed by a new immunoradiometric sandwich assay. Clin. Chem. 53, 284–291.

Kirino, Y., Yasukawa, T., Ohta, S., Akira, S., Ishihara, K., Watanabe, K., Suzuki, T., 2004. Codon-specific translational defect caused by a wobble modification deficiency in mutant tRNA from a human mitochondrial disease. Proc. Natl. Acad. Sci. U. S. A. 101, 15070–15075.

Koga, Y., Povalko, N., Katayama, K., Kakimoto, N., Matsuishi, T., Naito, E., Tanaka, M., 2012. Beneficial effect of pyruvate therapy on Leigh syndrome due to a novel mutation in PDH E1alpha gene. Brain Dev. 34, 87–91.

Lee, J.I., Dominy Jr., J.E., Sikalidis, A.K., Hirschberger, L.L., Wang, W., Stipanuk, M.H., 2008. HepG2/C3A cells respond to cysteine deprivation by induction of the amino acid deprivation/integrated stress response pathway. Physiol. Genomics 33, 218–229.

Li, J., Yang, L., Qin, W., Zhang, G., Yuan, J., Wang, F., 2013. Adaptive induction of growth differentiation factor 15 attenuates endothelial cell apoptosis in response to high glucose stimulus. PLoS One 8, e65549.

Lopez-Otin, C., Blasco, M.A., Partridge, L., Serrano, M., Kroemer, G., 2013. The hallmarks of aging. Cell 153, 1194–1217.

Martin, S.D., McGee, S.L., 2014. The role of mitochondria in the aetiology of insulin resistance and type 2 diabetes. Biochim. Biophys. Acta 1840, 1303–1312.

Pavlakis, S.G., Phillips, P.C., DiMauro, S., De Vivo, D.C., Rowland, L.P., 1984. Mitochondrial myopathy, encephalopathy, lactic acidosis, and strokelike episodes: a distinctive clinical syndrome. Ann. Neurol. 16, 481–488.

Rouschop, K.M., van den Beucken, T., Dubois, L., Niessen, H., Bussink, J., Savelkouls, K., Keulers, T., Mujcic, H., Landuyt, W., Voncken, J.W., Lambin, P., van der Kogel, A.J., Koritzinsky, M., Wouters, B.G., 2010. The unfolded protein response protects human tumor cells during hypoxia through regulation of the autophagy genes MAP1LC3B and ATG5. J. Clin. Invest. 120, 127–141.

Rzymski, T., Milani, M., Pike, L., Buffa, F., Mellor, H.R., Winchester, L., Pires, I., Hammond, E., Ragoussis, I., Harris, A.L., 2010. Regulation of autophagy by ATF4 in response to severe hypoxia. Oncogene 29, 4424–4435.

Saito, K., Kimura, N., Oda, N., Shimomura, H., Kumada, T., Miyajima, T., Murayama, K., Tanaka, M., Fujii, T., 2012. Pyruvate therapy for mitochondrial DNA depletion syndrome. Biochim. Biophys. Acta 1820, 632–636.

Sermeus, A., Michiels, C., 2011. Reciprocal influence of the p53 and the hypoxic pathways. Cell Death Dis. 2, e164.

Sperka, T., Wang, J., Rudolph, K.L., 2012. DNA damage checkpoints in stem cells, ageing and cancer. Nat. Rev. Mol. Cell Biol. 13, 579–590.

Suomalainen, A., Elo, J.M., Pietilainen, K.H., Hakonen, A.H., Sevastianova, K., Korpela, M., Isohanni, P., Marjavaara, S.K., Tyni, T., Kiuru-Enari, S., Pihko, H., Darin, N., Ounap, K., Kluijtmans, L.A., Paetau, A., Buzkova, J., Bindoff, L.A., Annunen-Rasila, J., Uusimaa, J., Rissanen, A., Yki-Jarvinen, H., Hirano, M., Tulinius, M., Smeitink, J., Tyynismaa, H., 2011. FGF-21 as a biomarker for muscle-manifesting mitochondrial respiratory chain deficiencies: a diagnostic study. Lancet Neurol. 10, 806–818.

Tanaka, M., Nishigaki, Y., Fuku, N., Ibi, T., Sahashi, K., Koga, Y., 2007. Therapeutic potential of pyruvate therapy for mitochondrial diseases. Mitochondrion 7, 399–401.

Teske, B.F., Wek, S.A., Bunpo, P., Cundiff, J.K., McClintick, J.N., Anthony, T.G., Wek, R.C., 2011. The eIF2 kinase PERK and the integrated stress response facilitate activation of ATF6 during endoplasmic reticulum stress. Mol. Biol. Cell 22, 4390–4405.

Tyynismaa, H., Carroll, C.J., Raimundo, N., Ahola-Erkkila, S., Wenz, T., Ruhanen, H., Guse, K., Hemminki, A., Peltola-Mjosund, K.E., Tulkki, V., Oresic, M., Moraes, C.T., Pietilainen, K., Hovatta, I., Suomalainen, A., 2010. Mitochondrial myopathy induces a starvation-like response. Hum. Mol. Genet. 19, 3948–3958.

Unsicker, K., Spittau, B., Krieglstein, K., 2013. The multiple facets of the TGF-beta family cytokine growth/differentiation factor-15/macrophage inhibitory cytokine-1. Cytokine Growth Factor Rev. 24, 373–384.

Welsh, J.B., Sapinoso, L.M., Kern, S.G., Brown, D.A., Liu, T., Bauskin, A.R., Ward, R.L., Hawkins, N.J., Quinn, D.I., Russell, P.J., Sutherland, R.L., Breit, S.N., Moskaluk, C.A., Frierson Jr., H.F., Hampton, G.M., 2003. Large-scale delineation of secreted protein biomarkers overexpressed in cancer tissue and serum. Proc. Natl. Acad. Sci. U. S. A. 100, 3410–3415.

Wiklund, F.E., Bennet, A.M., Magnusson, P.K., Eriksson, U.K., Lindmark, F., Wu, L., Yaghoutyfam, N., Marquis, C.P., Stattin, P., Pedersen, N.L., Adami, H.O., Gronberg, H., Breit, S.N., Brown, D.A., 2010. Macrophage inhibitory cytokine-1 (MIC-1/GDF15): a new marker of all-cause mortality. Aging Cell 9, 1057–1064.

Yang, H., Filipovic, Z., Brown, D., Breit, S.N., Vassilev, L.T., 2003. Macrophage inhibitory cytokine-1: a novel biomarker for p53 pathway activation. Mol. Cancer Ther. 2, 1023–1029.

Yasukawa, T., Suzuki, T., Ueda, T., Ohta, S., Watanabe, K., 2000. Modification defect at anticodon wobble nucleotide of mitochondrial tRNAs(Leu)(UUR) with pathogenic mutations of mitochondrial myopathy, encephalopathy, lactic acidosis, and stroke-like episodes. J. Biol. Chem. 275, 4251–4257.

Zhang, X.D., Qin, Z.H., Wang, J., 2010. The role of p53 in cell metabolism. Acta Pharmacol. Sin. 31, 1208–1212.

AUTHOR QUERY FORM

Journal: CMET

Article Number: 1726

Dear Author,

Please check your proof carefully and mark all corrections at the appropriate place in the proof.

Location in article	Query / Remark: Click on the Q link to find the query's location in text Please insert your reply or correction at the corresponding line in the proof
	There are no queries in this article

Thank you for your assistance.

Article

Cell Metabolism

Cdk5rap1-Mediated 2-Methylthio Modification of Mitochondrial tRNAs Governs Protein Translation and Contributes to Myopathy in Mice and Humans

Graphical Abstract

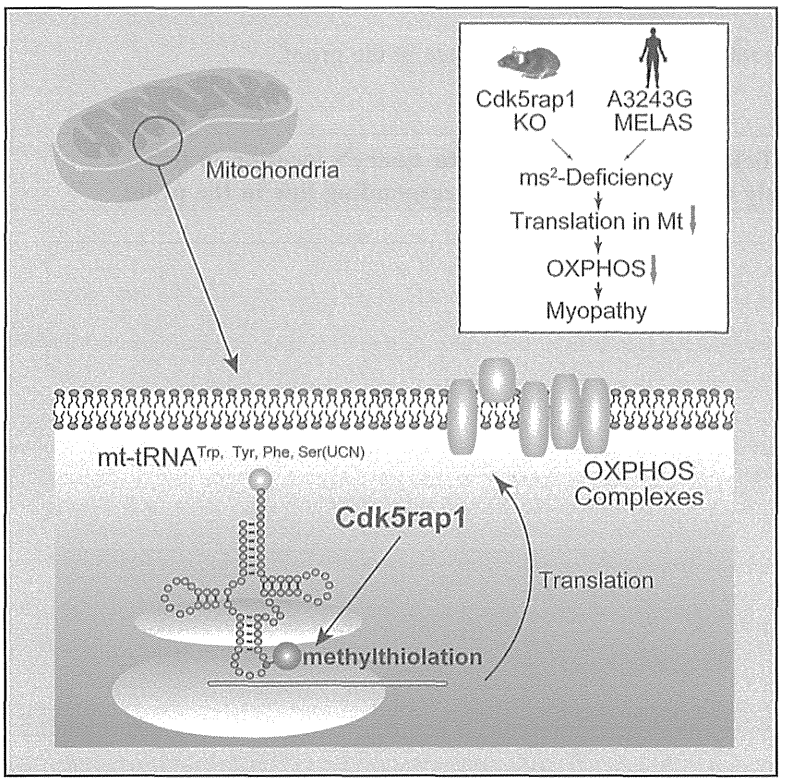

Authors

Fan-Yan Wei, Bo Zhou, ..., Yuichi Oike, Kazuhito Tomizawa

Correspondence

tomikt@kumamoto-u.ac.jp

In Brief

Wei et al. report that Cdk5rap1 is responsible for 2-methylthio (ms^2) modifications of mammalian mt-tRNAs. The modification is critical for efficient mitochondrial translation in mice and dysregulated in MELAS patients.

Highlights

- Cdk5rap1 catalyzes 2-methylthio (ms^2) modification of four mitochondrial tRNAs
- The ms^2 modifications optimize mitochondrial translation and OXPHOS activity
- Deficiency of ms^2 modification accelerates myopathy and cardiac dysfunction in mice
- The ms^2 modification levels are reduced in patients with mitochondrial disease

Wei et al., 2015, Cell Metabolism *21*, 1–15
March 3, 2015 ©2015 Elsevier Inc.
http://dx.doi.org/10.1016/j.cmet.2015.01.019

Please cite this article in press as: Wei et al., Cdk5rap1-Mediated 2-Methylthio Modification of Mitochondrial tRNAs Governs Protein Translation and Contributes to Myopathy in Mice and Humans, Cell Metabolism (2015), http://dx.doi.org/10.1016/j.cmet.2015.01.019

Cell Metabolism
Article

Cdk5rap1-Mediated 2-Methylthio Modification of Mitochondrial tRNAs Governs Protein Translation and Contributes to Myopathy in Mice and Humans

Fan-Yan Wei,[1,7] Bo Zhou,[1,7] Takeo Suzuki,[3] Keishi Miyata,[2] Yoshihiro Ujihara,[4] Haruki Horiguchi,[2] Nozomu Takahashi,[1] Peiyu Xie,[1] Hiroyuki Michiue,[5] Atsushi Fujimura,[5] Taku Kaitsuka,[1] Hideki Matsui,[5] Yasutoshi Koga,[6] Satoshi Mohri,[4] Tsutomu Suzuki,[3] Yuichi Oike,[2] and Kazuhito Tomizawa[1,*]

[1]Department of Molecular Physiology
[2]Department of Molecular Genetics
Faculty of Life Sciences, Kumamoto University, Kumamoto 860-8556, Japan
[3]Department of Chemistry and Biotechnology, School of Engineering, The University of Tokyo, Tokyo 113-8656, Japan
[4]First Department of Physiology, Kawasaki Medical School, Okayama 701-0192, Japan
[5]Department of Physiology, Okayama University Graduate School of Medicine, Dentistry and Pharmaceutical Sciences, Okayama 700-8558, Japan
[6]Department of Pediatrics and Child Health, Kurume University Graduate School of Medicine, Fukuoka 830-0011, Japan
[7]Co-first author
*Correspondence: tomikt@kumamoto-u.ac.jp
http://dx.doi.org/10.1016/j.cmet.2015.01.019

SUMMARY

Transfer RNAs (tRNAs) contain a wide variety of post-transcriptional modifications that are important for accurate decoding. Mammalian mitochondrial tRNAs (mt-tRNAs) are modified by nuclear-encoded tRNA-modifying enzymes; however, the physiological roles of these modifications remain largely unknown. In this study, we report that Cdk5 regulatory subunit-associated protein 1 (Cdk5rap1) is responsible for 2-methylthio (ms^2) modifications of mammalian mt-tRNAs for Ser(UCN), Phe, Tyr, and Trp codons. Deficiency in ms^2 modification markedly impaired mitochondrial protein synthesis, which resulted in respiratory defects in Cdk5rap1 knockout (KO) mice. The KO mice were highly susceptive to stress-induced mitochondrial remodeling and exhibited accelerated myopathy and cardiac dysfunction under stressed conditions. Furthermore, we demonstrate that the ms^2 modifications of mt-tRNAs were sensitive to oxidative stress and were reduced in patients with mitochondrial disease. These findings highlight the fundamental role of ms^2 modifications of mt-tRNAs in mitochondrial protein synthesis and their pathological consequences in mitochondrial disease.

INTRODUCTION

Transfer RNA (tRNA) is a key molecule in the translational apparatus to decode genetic information into proteins. A unique feature of tRNAs is the presence of a variety of chemical modifications of their nucleotides (Machnicka et al., 2013). These modifications are critical for efficient and accurate decoding (Agris, 2004; Suzuki, 2005). To date, more than 100 modified nucleotides have been identified in tRNAs from the three domains of life, indicative of the universal importance of tRNA modifications (Machnicka et al., 2013).

Given the critical roles of tRNA modifications in cells, it is not surprising that tRNA modification deficiencies have been associated with human diseases (Torres et al., 2014). Genetic variations in the gene encoding Cdk5 regulatory subunit associated protein 1-like-1 (CDKAL1), which inserts a 2-methylthio (ms^2) group into the N^6-threonylcarbamoyl adenosine (t^6A) of cytosolic $tRNA^{Lys}$(UUU), have been associated with the development of type 2 diabetes (Steinthorsdottir et al., 2007; Arragain et al., 2010). A deficiency in the ms^2 modification of $tRNA^{Lys}$(UUU) resulted in aberrant proinsulin synthesis, which ultimately led to impaired glucose metabolism and insulin secretion in Cdkal1 knockout (KO) mice and in human subjects carrying T2D-associated alleles of *CDKAL1* (Wei et al., 2011; Xie et al., 2013).

In mitochondrial tRNAs (mt-tRNAs), 15 species of modified nucleotides at 118 positions have been identified in bovine (Suzuki and Suzuki, 2014). Some of these modifications have been associated with the development of mitochondrial diseases, such as Mitochondrial myopathy, encephalopathy, lactic cidosis, stroke-like episodes (MELAS), and myoclonus epilepsy with ragged-red fibers (MERRF) (Suzuki et al., 2011). mt-$tRNA^{Leu}$ and mt-$tRNA^{Lys}$ contain 5-taurinomethyl (τm^5) and 5-taurinomethyl-2-thio ($\tau m^5 s^2$) modifications, respectively, at U34 (Yasukawa et al., 2001; Suzuki et al., 2002), and both of these modifications are critical for decoding their cognate codons (Kirino et al., 2004; Yasukawa et al., 2001). The absence of these modifications has been observed in MELAS patients carrying the A3243G mutation in mt-$tRNA^{Leu}$ and in MERRF patients carrying the A8344G mutation in mt-$tRNA^{Lys}$ (Yasukawa et al., 2001). These results suggest a critical role for mt-tRNA modifications in the pathogenesis of human diseases. Nevertheless, knowledge regarding the physiological roles of tRNA modifications is incomplete, and a complete investigation of the individual types of mt-tRNA modifications is required to fully understand the physiological function and molecular pathology of tRNA modifications in human diseases.

In mammalian mt-tRNAs, 2-methylthio-N^6-isopentenyl adenosine (ms^2i^6A) is a unique modification that is conserved in all three domains of life (Machnicka et al., 2013). In bacteria, the ms^2 modification of ms^2i^6A contributes to accurate decoding by improving tRNA binding to codons (Urbonavicius et al., 2001; Jenner et al., 2010). However, the physiological importance of ms^2 modifications in mammals is unknown. We have previously shown that Cdk5rap1 might be responsible for the ms^2 modification of ms^2i^6A because of its homology to Cdkal1, which catalyzes ms^2t^6A modification (Arragain et al., 2010). Recently, Cdk5rap1 was proposed to catalyze ms^2 group insertion in both cytosolic RNAs and mt-tRNAs; however, the exact substrate tRNA of Cdk5rap1 in mammalian cells remains unclear (Reiter et al., 2012).

Given the exclusive mitochondrial localization of ms^2i^6A in mammals and the implication of this localization in the decoding process, we hypothesize that Cdk5rap1 might specifically catalyze the ms^2 modification of mt-tRNAs and contribute to mitochondrial function in vivo. In this study, we validated this hypothesis through a thorough investigation of the physiological function of the ms^2 modification in Cdk5rap1 KO mice. Furthermore, we investigated the pathological implication and the molecular mechanism of the ms^2 modification in MELAS patients.

RESULTS

Cdk5rap1 Catalyzes the Conversion of i^6A to ms^2i^6A in Mitochondrial tRNAs

Based on the high homology between mammalian Cdk5rap1 and bacterial MiaB, we and another group previously showed that Cdk5rap1 might be a mammalian methylthiotransferase that catalyzes the conversion of N^6-isopentenyl adenosine (i^6A) to 2-methylthio-N^6-isopentenyl adenosine (ms^2i^6A) (Figure 1A and see Figure S1A available online; Arragain et al., 2010; Reiter et al., 2012). To investigate this hypothesis, we transformed Cdk5rap1 in MiaB-deficient bacteria (ΔMiaB), which do not contain ms^2 modifications. As expected, the transformation of Cdk5rap1 restored ms^2 modifications (Figure 1B). The conserved cysteine residues in the UPF domain and the radical SAM domain of MiaB are critical for ms^2 modification through their interaction with two [4Fe-4S] clusters (Forouhar et al., 2013). Similar to MiaB, the mutation of cysteine residues in the UFP domain or the radical SAM domain of Cdk5rap1 completely abolished the ms^2 modification (Figure 1B).

To prove that Cdk5rap1 is a mitochondrial methylthiotransferase and to identify its exact substrates, we generated Cdk5rap1 KO mice (Figures S1B–S1D). As expected, the ms^2 modification was completely abolished in KO mice (Figures S1E and S1F). Cdk5rap1 colocalized with Mitotracker in HeLa cells (Figure S2A). Cdk5rap1 with a deletion of mitochondrial localization signal at the N terminus exhibited cytosolic localization but retained its enzyme activity (Figures S2A and S2B). However, no ms^2 modification was detected in Cdk5rap1-deficient mouse embryonic fibroblast (MEF) cells expressing the cytosolic form of Cdk5rap1 (Figures S2C and S2D). These results indicate that Cdk5rap1 localizes on mitochondria and specifically modifies mt-tRNAs. To identify the exact substrate of Cdk5rap1, individual mt-tRNA was isolated from WT and KO mice and subjected to mass spectrometric analysis. The ms^2 modification was completely absent at A37 in mt-$tRNA^{Phe}$, mt-$tRNA^{Trp}$, mt-$tRNA^{Tyr}$, and mt-$tRNA^{Ser(UCN)}$ isolated from KO mice (Figures 1C–1F). The absence of an ms^2 modification did not affect the nearby τm^5 modification at U34 in mt-$tRNA^{Trp}$ (Figure S1F). These results clearly demonstrate that Cdk5rap1 is a two [4Fe-4S] cluster-containing mitochondrial methylthiotransferase that specifically converts i^6A to ms^2i^6A at A37 of mt-$tRNA^{Phe}$, mt-$tRNA^{Trp}$, mt-$tRNA^{Tyr}$, and mt-$tRNA^{Ser(UCN)}$ in mammalian cells.

The ms^2 Modification Controls Codon-Specific Decoding Fidelity in a Translation Rate-Dependent Manner

A previous study demonstrated that the ms^2 group of 2-methylthio-N^6-hydroxyisopentenyl adenosine (ms^2io^6A) is critical for the accurate decoding of Tyr and Phe codons (Urbonavicius et al., 2001). To thoroughly investigate the role of ms^2 modifications of tRNAs during the decoding of their cognate codons, we utilized a luciferase-based reporter and transformed the plasmid into a WT strain or the ΔMiaB strain to detect frameshifting in the presence or absence of the ms^2 modification. The firefly luciferase gene was properly translated only when frameshifting occurred at the cognate codons read by $tRNA^{Phe}$, $tRNA^{Trp}$, $tRNA^{Tyr}$, or $tRNA^{Ser(UCN)}$ (Figure S2E). A deficiency in ms^2 modification induced frameshifting at Phe(TTT) and Tyr(TAT) codons (Figure 1G). Induction of protein translation by isopropyl-beta-D-thiogalactopyranoside (IPTG) exaggerated the overall frameshifting rate in both the WT and ΔMiaB strains. In addition to the Phe(TTT) and Tyr(TAT) codons, there was a significant increase in ms^2-dependent frameshifting at the Tyr(TAC), Ser(TCT), Ser(TCC), and Ser(TCG) codons, for which frameshifting was not observed without IPTG induction (Figures S1G–S1I). Importantly, these results show that ms^2-dependent frameshifting specifically occurred during the translation of wobble codons, such as Phe(TTT), Tyr(TAT), Ser(TCT), Ser(TCC), and Ser(TCG), with the exception of the Tyr(TAC) codon, but not the cognate codons, such as Phe(TTC), Ser(TCA), and Trp(TGG) (shown in red in Figures S1F–S1I). Furthermore, the ms^2-deficiency-evoked frameshifting was fully reversed by transformation with active Cdk5rap1, but not dominant-negative Cdk5rap1 (Figure 1G). These results demonstrate that ms^2 modification is critical for the accurate decoding of wobble codons corresponding to $tRNA^{Phe}$, $tRNA^{Tyr}$, or $tRNA^{Ser(UCN)}$ in a translation rate-dependent manner.

Deficiency of the Mitochondrial ms^2 Modification Attenuates Mitochondrial Translation

To examine mitochondrial protein synthesis, WT or KO MEF cells were labeled with ^{35}S-methionine for 1 hr and subjected to pulse chase. The mitochondrial protein synthesis was substantially decreased in KO MEF cells (Figure 2A). Furthermore, MEF cells were radioactively labeled and subjected to blue native PAGE to examine the formation of respiratory complexes. The incorporation of mitochondrial proteins into complexes I, III, and IV was substantially decreased in KO MEF, whereas complex V was unaffected (Figures 2B and 2C). These results suggest that the deficiency in ms^2 modification greatly attenuated mitochondrial protein synthesis, resulting in impaired complex assembly.

The maintenance of mitochondrial OXPHOS subunits is critical for the electron transport chain, which maintains the resting

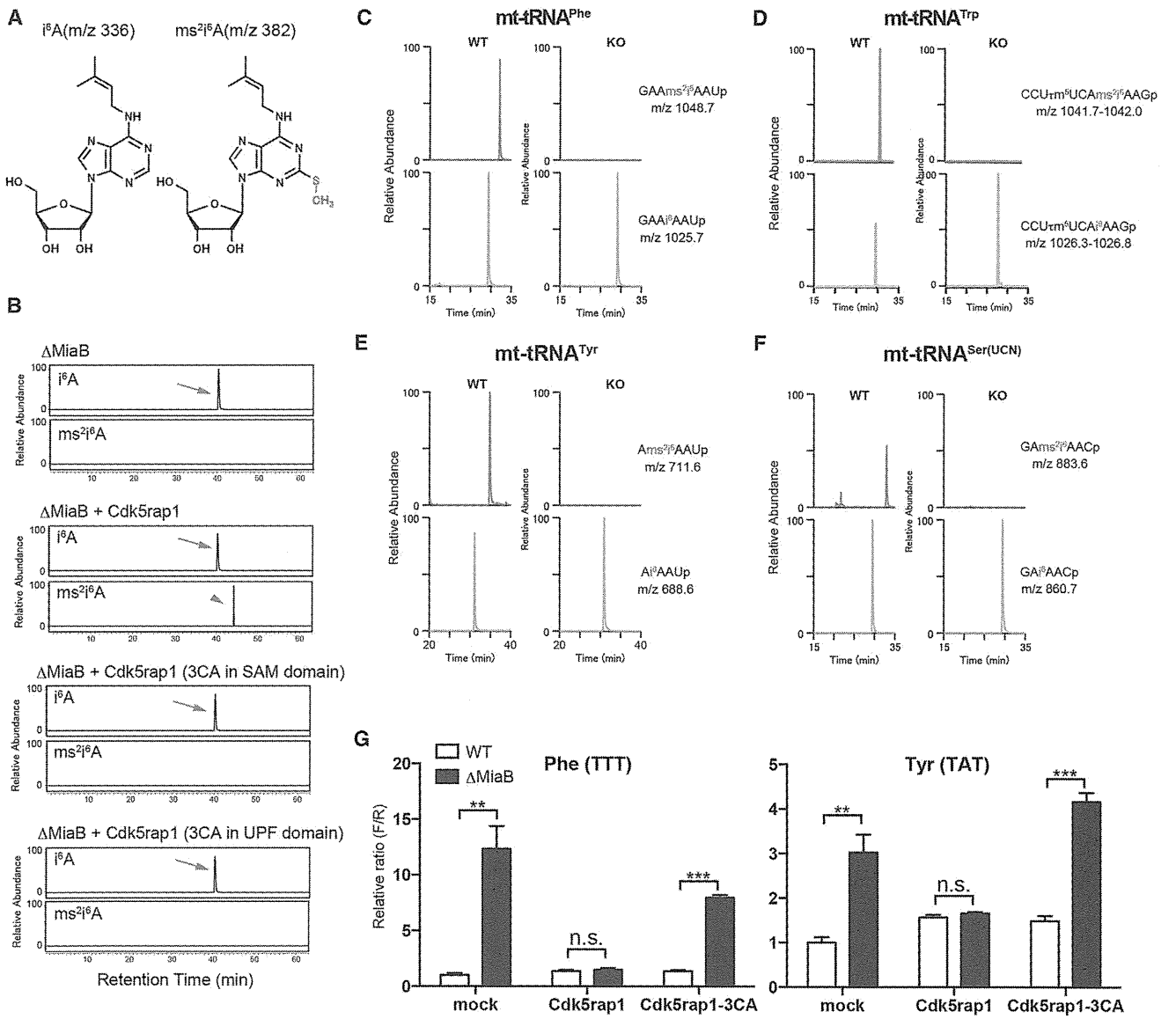

Figure 1. Cdk5rap1 Is The Mammalian mt-tRNA Methylthiotransferase

(A) Structures of N^6-isopentenyladenosine (i^6A) and 2-methylthio-N^6-isopentenyladenosine (ms^2i^6A) and the corresponding m/z values are shown. The ms^2 group ($S\text{-}CH_3$) is shown in red.

(B) GST-Cdk5rap1 or GST-Cdk5rap1 with Cys-to-Ala mutations (3CA) was transformed into the MiaB-deficient strain (ΔMiaB). The arrows and arrowhead indicate the peaks corresponding to i^6A and ms^2i^6A, respectively.

(C–F) Examination of the ms^2i^6A modification in mt-$tRNA^{Phe}$ (C), mt-$tRNA^{Trp}$ (D), mt-$tRNA^{Tyr}$ (E), and mt-$tRNA^{Ser(UCN)}$ (F) isolated from WT and KO mice by mass spectrometry. The mass chromatograms show the peaks corresponding to fragments containing i^6A or ms^2i^6A.

(G) Frameshifting assay. WT and ΔMiaB bacteria were transformed with Cdk5rap1 or inactive Cdk5rap1 (Cdk5rap1-3CA). The relative ratio of firefly luciferase activity to renilla luciferase activity (F/R) represents the decoding error. n = 4. Data are mean ± SEM. **p < 0.01, ***p < 0.0001.

mitochondrial membrane potential and drives respiration. We thus investigated the mitochondrial membrane potential in WT and KO MEF cells. There was a marked increase in cell populations with very low membrane potential in KO MEF cells (Figure 2D). Consequently, the oxygen consumption rate in KO cells was significantly lower than that in WT MEF cells (Figure 2E). Furthermore, the KO cells quickly lost their mitochondrial membrane potential after treatment with very low doses of rotenone and FCCP, which had little effect on WT cells (Figures 2F and 2G). These results thus demonstrate that ms^2 modifications of mt-tRNAs are critical for maintaining efficient mitochondrial translation and respiratory chain.

Deficiency of Mitochondrial ms^2 Modification Impairs OXPHOS in Skeletal Muscle and Heart Tissue without Affecting Basal Metabolism

To investigate the physiological role of mitochondrial ms^2 modification, we examined the phenotype of KO mice in vivo. Despite

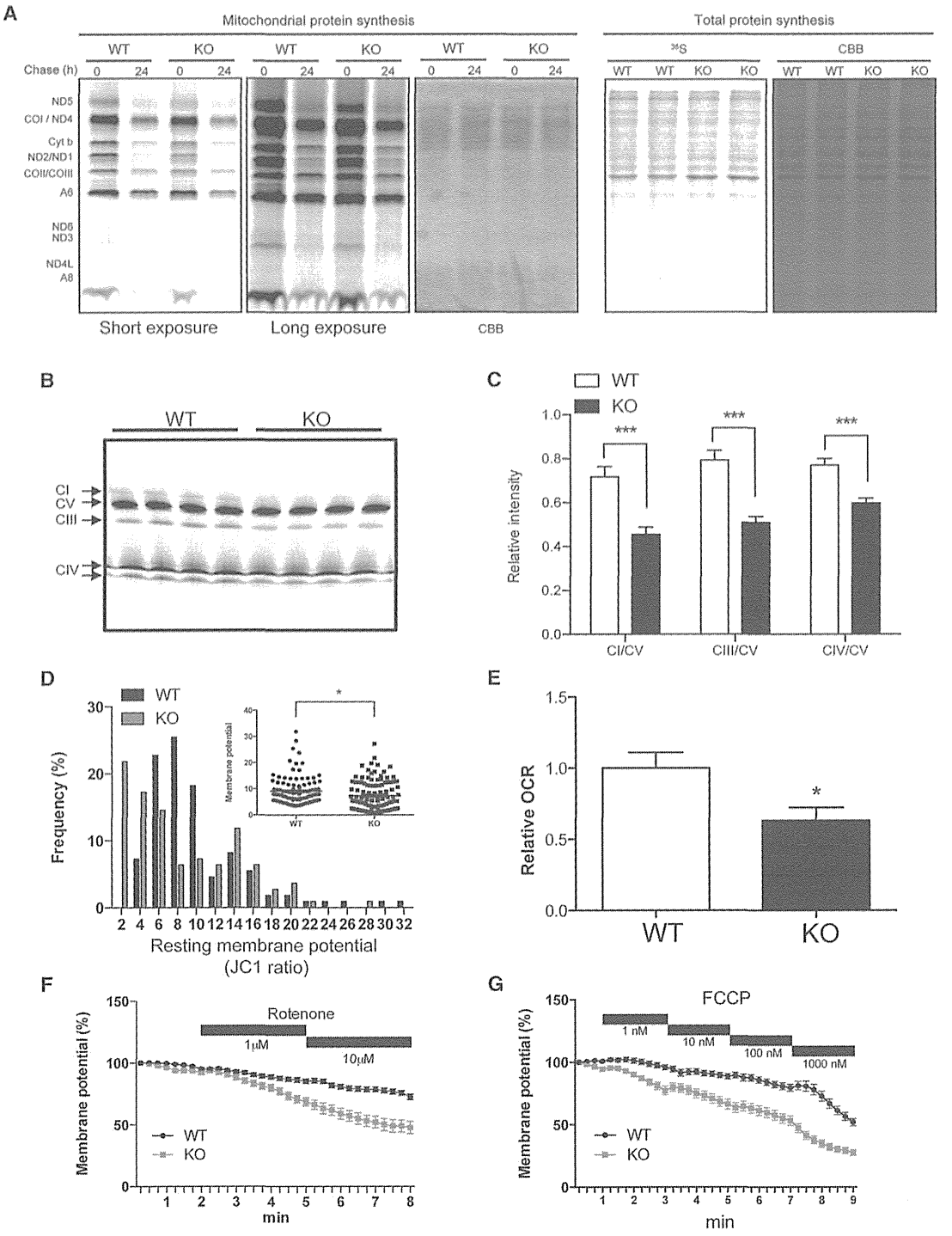

Figure 2. Deficiency in the ms^2 Modifications Impaired Mitochondrial Protein Synthesis and Mitochondrial Functions

(A) WT and KO MEF cells were labeled with ^{35}S-Met/Cys and chased for 0 or 24 hr in the presence of emetine for measurement of mitochondrial protein synthesis (left panels). MEF cells were labeled with ^{35}S-Met/Cys for 1 hr, and total protein synthesis was measured (right panels). CBB staining of gel was used as loading control.

(B and C) The autoradiogram of blue native PAGE shows a decrease in the incorporation of mitochondrial proteins in complexes I, III, and IV in KO MEF cells (B). The relative intensity of complex I, III, and IV versus complex V was quantified (C).

(D) The histogram and inserted graph show that KO MEF cells contain a number of mitochondria with low membrane potentials; n = 110 each.

(E) KO cells showed a significant decrease in the oxygen consumption rate (OCR); n = 10 each.

(E–G) Cells were stained with TMRM for measuring membrane potential. The relative membrane potential in the presence of rotenone (F) or FCCP (G) was analyzed; n = 66 for WT and n = 30 for KO (F); n = 43 for WT and n = 32 for KO (G). Data are mean ± SEM. *p < 0.05.

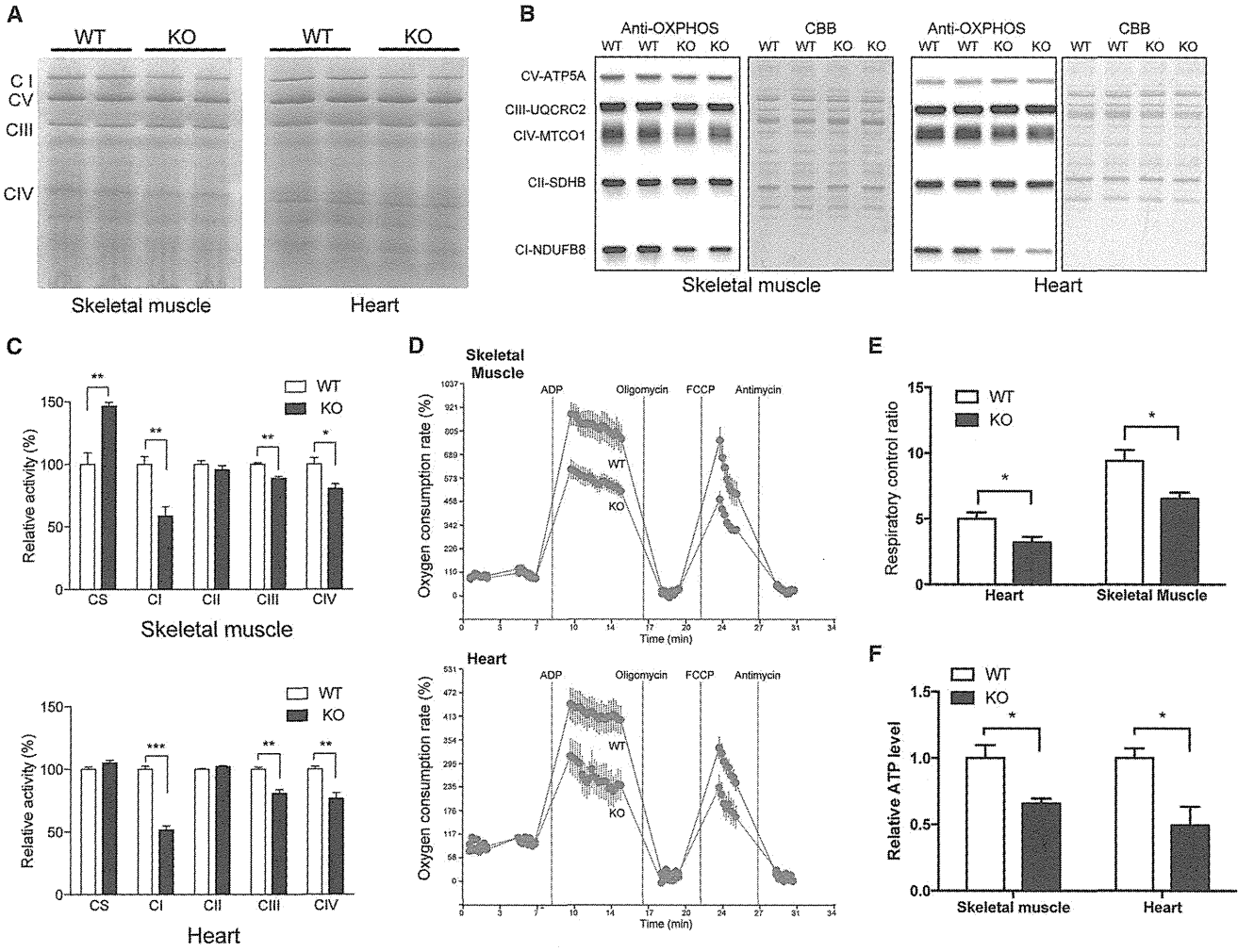

Figure 3. The Deficiency in ms^2 Modification Impaired Mitochondrial Function In Vivo

(A) Steady-state levels of complex I (CI), complex II (CIII), complex IV (CIV), and complex V (CV) in mitochondria isolated from skeletal muscle and heart tissues were examined by BN-PAGE.

(B) Steady-state levels of representative proteins of CI-CIV were examined by western blotting. CBB staining was used as loading control.

(C) The activities of CS, CI-CIV in skeletal muscle (left panel), and heart (right panel) of WT and KO mice were examined. n = 4–5.

(D and E) Respiratory coupling was decreased in Cdk5rap1-deficient mitochondria isolated from skeletal muscle and heart tissue when examined using XF24 Flux Analyzer; n = 4–5.

(F) The steady-state levels of ATP in the skeletal muscle and heart tissue of WT and KO mice were examined; n = 4 each. Data are mean ± SEM. *p < 0.05.

the mitochondrial dysfunction in KO cells, the Cdk5rap1 KO mice developed normally without obvious morphological changes in major tissues (Figures S3A and S3B). The energy expenditure and glucose metabolism in KO mice were compatible with those of WT mice (Figures S3C–S3E). Furthermore, there was no difference in neurological behaviors between KO and WT mice (Figures S3F–S3I).

Of all tissues, skeletal muscle and heart tissue are the most susceptible tissues to mitochondrial dysfunction (DiMauro and Schon, 2003). We therefore closely examined these two tissues in KO mice. Substantial decreases in the steady-state levels of complex I and IV were observed in both skeletal muscle and heart tissues of KO mice compared with WT mice, with complex I being markedly affected (Figure 3A). Accordingly, the steady-state levels of complex I and IV proteins, such as NDUFB8 and MTCO1, respectively, were markedly decreased in skeletal muscle and heart tissues of KO mice compared with WT mice (Figure 3B). As a result, complex I activity was significantly impaired in KO mice (58.6% of WT for skeletal muscle and 51.5% of WT for heart tissue) (Figure 3C). There was a mild but significant decrease in complex III and complex IV activity in KO mice (muscle: complex III, 88.8% of WT; complex IV, 80.5% of WT; heart: complex III, 80.7% of WT, complex IV, 79.8% of WT) (Figure 3C). The decrease in mitochondrial activity in the skeletal muscle of KO mice was also confirmed by cytochrome oxidase (COX) staining (Figure S3J). Accordingly, the oxygen consumption elicited by ADP and FCCP in Cdk5rap1-deficient mitochondria was significantly lower than that in WT mitochondria, indicating that electron transport and respiratory coupling were impaired in the skeletal muscle and heart tissue of KO mice (respiratory

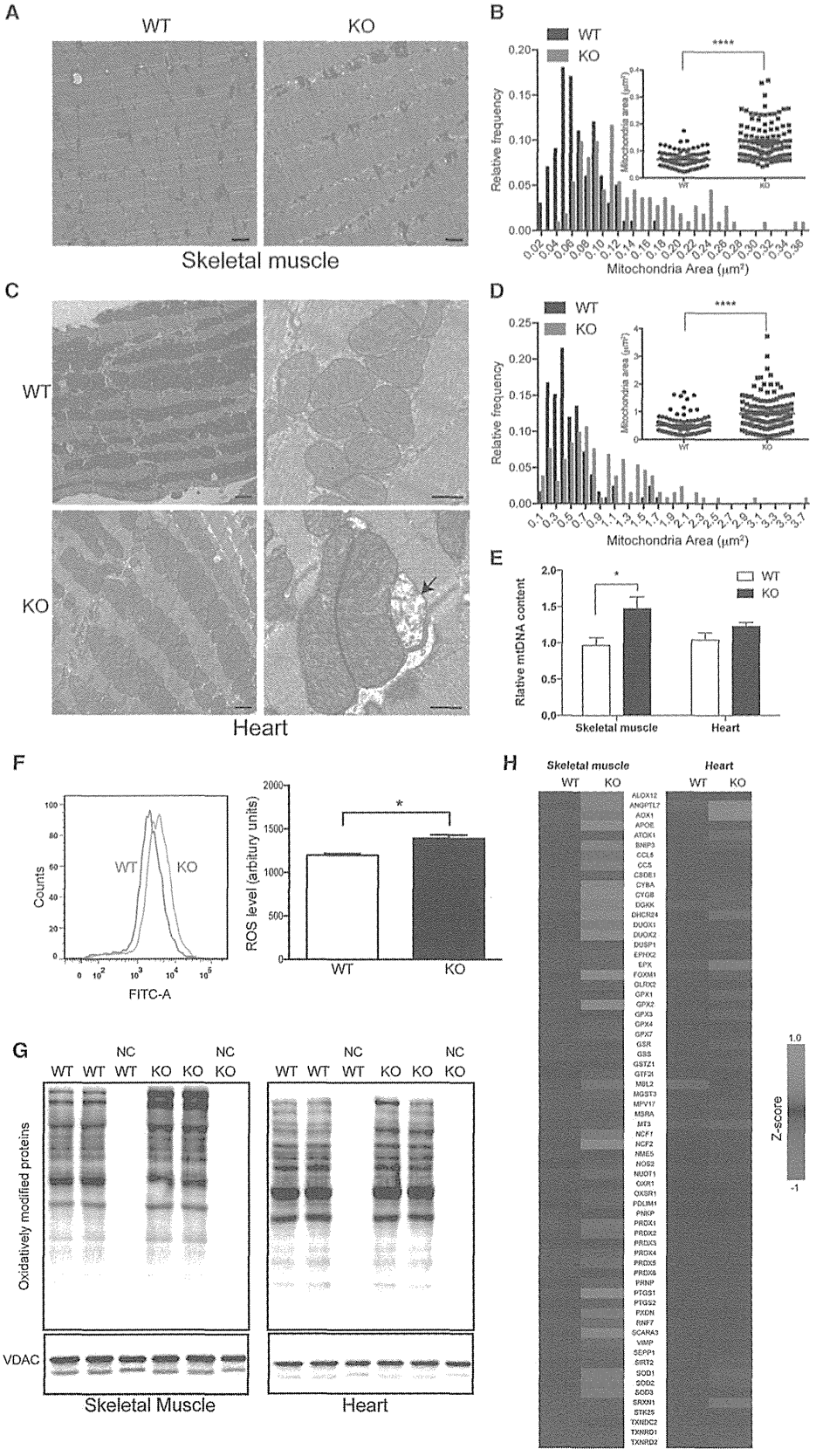

(legend on next page)

control ratio of the hearts of WT and KO: 4.9 and 3.2, skeletal muscles of WT and KO: 9.4 and 6.5, respectively; Figures 3D and 3E). Consequently, the steady-state ATP level in skeletal muscle and heart tissue of KO mice was lower than that in WT mice (Figure 3F).

Impairment of mitochondrial function usually exaggerates mitochondrial remodeling as a compensation mechanism. There was an increase in the mitochondrial mass in the skeletal muscle of KO mice as examined by electron microscopy and Gomori Trichrome staining (Figures 4A, 4B, and S3J). Strikingly, the mitochondrial was abnormally enlarged in heart tissue of KO mice (Figures 4C and 4D). A progressive disruption of cristae was occasionally observed in the mitochondria of the cardiac muscle of KO mice (arrow in Figure 4C). Furthermore, there was a significant increase in citrate synthase activity (Figure 3C) as well as relative mtDNA content (Figure 4E) in the skeletal muscle of KO mice.

Reactive oxygen species (ROS) are byproducts of mitochondrial electron transport and mainly generated from complexes I and III (Murphy, 2009). A deficiency of complexes I and III accelerates the leakage of ROS from electron transport chain and contributes to the development of mitochondrial diseases. Given the marked decrease in complex I protein level in KO mice, we investigated ROS production in KO mice (Figure 4F). The ROS level was slightly but significantly higher in KO MEF cells than that in WT MEF cells. This finding was corroborated by a moderate increase in protein carbonylation (Figure 4G) as well as oxidative stress-related gene expression in both skeletal muscle and heart tissues of KO mice (Figure 4H).

To further investigate the impact of deficiency of ms^2 modification on physiological function, we examined muscular and cardiac function in vivo. However, the treadmill performance of KO mice was comparable with that of WT mice (Figure S3K). The echocardiography examination indicated that no apparent cardiac defects were present in the KO mice (Figure S3L). Taken together, these results demonstrate that the deficiency of ms^2 modifications in mt-tRNAs impairs mitochondrial protein synthesis, which leads to a reduction of respiratory activity and increase in ROS in skeletal muscle and heart tissue. However, considering the overall phenotypes, mice seem to tolerate an up to 50% reduction of complex I activity due to the loss of ms^2 modifications under sedentary conditions.

Loss of ms^2 Modifications Accelerates OXPHOS Defects under Stressed Conditions

The mild phenotype of KO mice prompted us to challenge the mice with a ketogenic diet (KD; very high fat and ultra-low carbohydrate). Ketone bodies from KD bypass glycolysis and generate energy mostly through fatty acid oxidation in mitochondria (Laffel, 1999). Adaptation to this metabolic pressure is accompanied by mitochondrial rearrangement (Grimsrud et al., 2012). Therefore, it is conceivable that the accurate regulation of mitochondrial protein synthesis by ms^2 modification is particularly important for mitochondrial remodeling under stressed conditions.

As expected, KD treatment accelerated OXPHOS defects in the skeletal muscle and heart tissue of KO mice (Figures 4A and 4B). Complex I activity was significantly impaired in KD-fed KO mice (48.6% of the KD-fed WT for skeletal muscle and 47.7% of the KD-fed WT for heart tissue) (Figures 5A and 5B). In addition, accelerated decreases in complex III and IV activities were observed in the KD-fed KO mice (muscle: complex III, 82.9% of the KD-fed WT; complex IV, 62.9% of the KD-fed WT; heart: complex III, 75% of the KD-fed WT; complex IV, 57.8% of the KD-fed WT).

The OXPHOS defect after KD treatment exaggerated the mitochondrial remodeling pathway in both WT and KO mice. There was a ~3-fold and ~1.5-fold increase in mtDNA content in the skeletal muscle and heart tissue of both WT and KO mice fed a KD, respectively (Figure 5C). However, there was no difference in the mtDNA content in skeletal muscle and heart tissue between WT and KO mice (Figure 5C). Accordingly, subsequent electron microscopic examination revealed a marked increase in mitochondria mass (Figures 5D and 5F). In the skeletal muscles of KO mice fed a KD, mitochondrial proliferation was observed in both intermyofibrillar and subsarcolemmal mitochondria, with the latter drastically increased (Figure 5D). Importantly, KD-fed KO mice exhibited a considerable population of mitochondria with disrupted cristae in the skeletal muscle tissue (arrowheads in Figure 5D). The enlargement of mitochondria and the disruption of cristae were even more prominent in the heart tissue of KO mice fed a KD (arrows in Figure 5D). These results demonstrate that Cdk5rap1-dependent ms^2 modification is crucial for the maintenance of OXPHOS activity and mitochondrial morphology under stress.

The acceleration of the OXPHOS defect in KO mice may be due to the indirect lipotoxicity from the very high-fat diet. However, the body weight and serum metabolic profiles of KO mice fed a KD were the same as those of WT mice fed a KD (Figures S4A–S4C). There was no difference in the locomotor activity or energy expenditure between the WT and KO mice fed a KD (Figures S4D and S4E). Interestingly, the glucose level in the KD-fed KO mice was somewhat lower than that in the KD-fed WT mice (Figure S4F). Taken together, these results indicate that the progressive OXPHOS defects and mitochondrial degeneration in KD-fed KO mice directly resulted from a deficiency in Cdk5rap1-dependent ms^2 modification during mitochondrial remodeling.

Figure 4. Aberrant Mitochondrial Morphology and ROS Metabolism in KO Mice

(A–D) Mitochondria in skeletal muscle and heart tissue were examined by electron microscopy. KO mice exhibit disrupted mitochondrial morphology (A and C) and increased mitochondrial mass (B and D). Bars in (A) and the left panels of (C), 10 μm. Bars in the right panels of (C), 0.5 μm. WT, n = 100; KO, n = 112 in (B) and n = 126; KO, n = 132 in (D).

(E) The relative contents of mtDNA in muscle and heart tissue were examined; n = 6–9.

(F) ROS levels were analyzed by measuring the florescent intensity of CM-H2DCFDA in WT and MEF cells (left panel). The intensity was quantified (right panel); n = 3.

(G) Protein carbonylation levels were increased in the mitochondria of skeletal muscle and heart tissue in KO mice.

(H) Heatmap showing the differentially regulated genes involved in oxidative stress response in skeletal muscle and heart tissue of WT and KO mice; n = 4. Data are mean ± SEM. *p < 0.5, ****p < 0.0001.

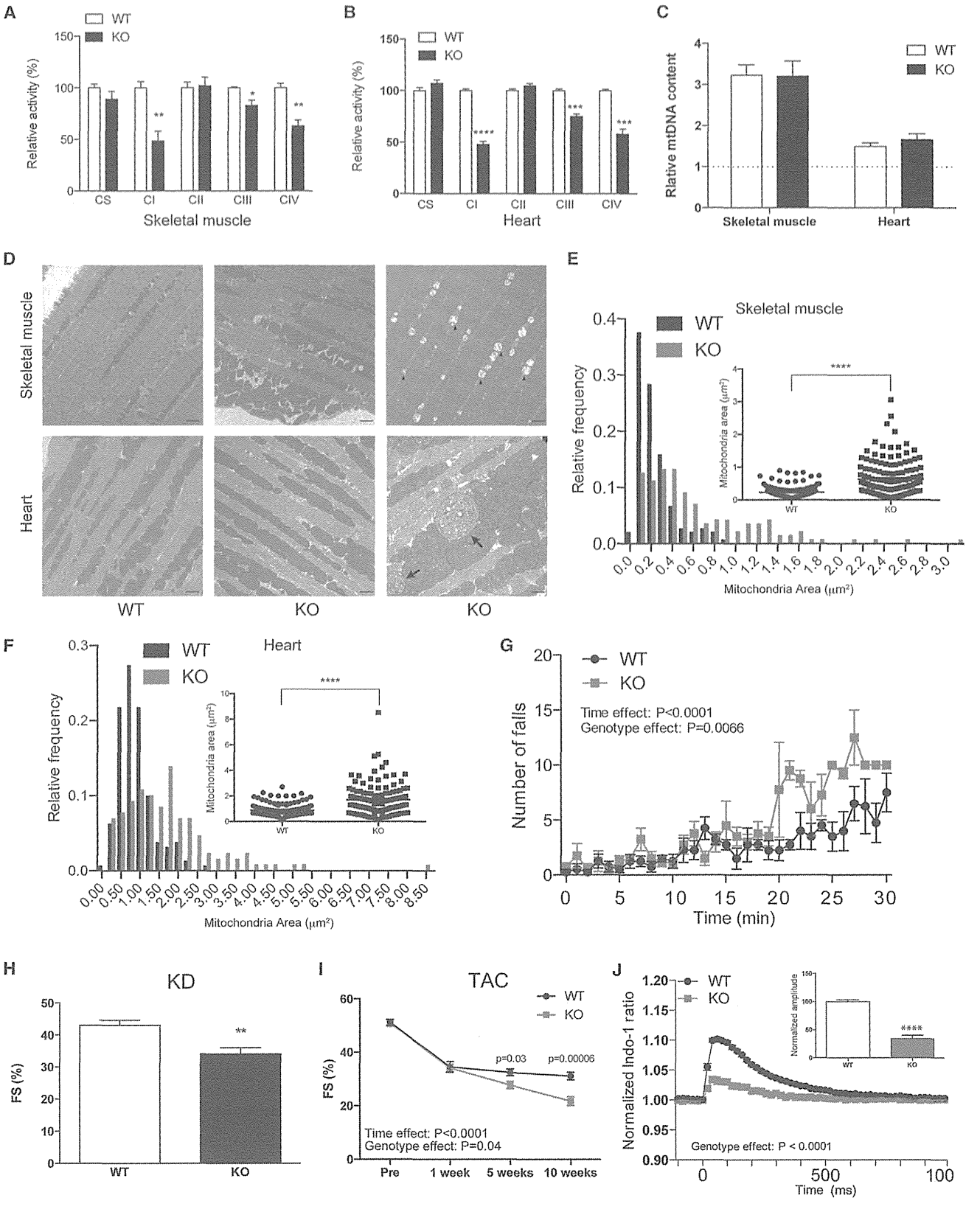

(legend on next page)

Loss of ms^2 Modification Accelerates Muscular and Cardiac Dysfunction under Stress

The KD-induced OXPHOS defect markedly accelerated the dysfunction of skeletal muscle and heart tissue in the KO mice. In a treadmill test, KO mice fed a KD showed a significant increase in the number of falls and became exhausted as early as 30 min into the test (Figure 5G). The KO mice also showed moderate cardiac hypertrophy, as indicated by an increase in heart volume, heart weight, and left ventricle posterior wall thickness (Figures S5A–S5C). The percentage of fractional shortening (FS%) in KO mice fed a KD was significantly lower than that in WT mice fed a KD (WT, 43% versus KO, 34%; Figure 5H). In addition to a KD-induced stress model, we utilized a transverse aortic constriction (TAC) model, which is a standard model for inducing cardiac dysfunction by pressure overload. Because the TAC model is also accompanied by global mitochondrial remodeling (Dai et al., 2012), we expected that a deficiency in ms^2 modification would further accelerate cardiac dysfunction. Indeed, chronic TAC resulted in a progressive cardiac hypertrophy, as indicated by an increase in heart weight and left ventricle posterior wall thickness in KO mice (WT, 7.5 mg/g body weight; KO, 11.3 mg/g body weight; Figures S5A and S5D–S5F). In WT mice, the FS% dropped from 51.2% to 34.5% 1 week after TAC but was then maintained until 10 weeks (5 weeks, 32.4; 10 weeks, 31.1; Figure 5I). In contrast, the FS% in KO mice continuously decreased after TAC and eventually decreased to as low as 21.7% (Figure 5I). Further examination in isolated cardiomyocytes revealed that the cardiac dysfunction observed in the TAC model of KO mice was associated with a decrease in calcium influx and contraction rate (Figures 5J and S5G). These results demonstrate that a deficiency of the ms^2 modifications in mt-tRNAs can cause a catastrophic defect in muscle and heart tissue under stressed conditions.

Deficiencies in ms^2 Modification Compromise the Quality of Mitochondria

Next, we investigated the molecular mechanism underlying the stress-induced acceleration of OXPHOS defects and cardiomyopathy in KO mice. Adaptation to mitochondrial stress requires coordinated protein synthesis (Dai et al., 2012). Because ms^2 modification controls decoding fidelity in a translation-rate-dependent manner, it is conceivable that a deficiency in ms^2 modification under stressed conditions might markedly compromise mitochondrial quality as well as integrity, which would result in severe OXPHOS defects and ultimately lead to myopathy and cardiac dysfunction. Indeed, a moderate increase in the complex I level was observed in WT mice treated with KD or TAC surgery (Figures 6A and 6B). In contrast, the steady-state levels of complexes I and IV levels were somewhat decreased in KD-fed and TAC KO mice when compared with NC-fed KO mice. The mitochondrial stresses increased protein carbonyltaion in both WT and KO mice. As a result, the protein carbonylation level in stressed heart tissues of KO mice was moderately higher than that in the stressed WT mice (Figure S6A). Impaired mitochondrial proteostasis exaggerates mitochondrial unfolded protein response (mt-UPR) (Durieux et al., 2011; Houtkooper et al., 2013). Accordingly, proteins involved in mtUPR, such as Yme1l1, Afg3l2, and Lonp1, were upregulated in mitochondria isolated from the hearts of KO mice treated with KD and TAC compared with WT mice (Figure 6C). Furthermore, a marked increase in polyubiquitinated proteins was observed in mitochondria isolated from the hearts of KO mice under stressed conditions (Figure 6D). Interestingly, the levels of polyubiquitination were proportional to the levels of cardiac function (FS%) in stressed KO mice (TAC > KD > NC; Figure 6D; also see Figures 5H and 5I).

Mitophagy is the hallmark of the existence of compromised mitochondria. Parkin, an E3 ubiquitin ligase, primes mitophagy by translocation to mitochondria with low membrane potentials and ubiquitination of mitochondrial proteins (Kubli and Gustafsson, 2012). Because cells with ms^2 modification deficiencies had a low basal mitochondrial membrane potential and were susceptible to stress-induced depolarization (Figures 2F and 2G), we hypothesized that mitochondrial stress might exaggerate the recruitment of Parkin to mitochondria and the acceleration of mitophagy in Cdk5rap1 KO cells. In KO cells treated with FCCP, most of the Parkin translocated to the mitochondria as soon as 2 hr after treatment, whereas similar translocation was not observed in WT cells treated with FCCP (Figure 6E; also see the separated imaged in Figure S6B). A number of large mitochondrial aggregates were surrounded by the autophagosomal membrane protein LC3 in KO cells treated with FCCP, which is indicative of acceleration of mitophagy (Figure 6F; also see the separated imaged in Figure S6C). Furthermore, we observed a number of degenerated mitochondria, with some mitochondria being degraded in autophagic vacuoles in KD-fed and TAC KO mice, by electron microscopic examination (Figure 6G). These

Figure 5. Mitochondrial Stresses Accelerated Myopathy and Cardiac Dysfunction in ms^2-Deficient Mice

(A and B) WT and KO mice at 8 weeks old were fed for KD for 10 weeks. The relative activities of CS, CI-CIV in skeletal muscle (A), and heart (B) were examined; n = 5–7 each.

(C) The relative mtDNA contents in skeletal muscle and heart tissue of KD-fed WT and KO mice were examined; n = 6–7. The dashed lines represent the relative mtDNA content in NC-fed WT mice.

(D–F) Electron microscopy examination of skeletal muscle and heart tissue show disrupted mitochondrial architecture (D) and a marked increase in mitochondrial mass (E and F) in KD-fed KO mice. Arrowheads and arrows indicate mitochondria with abnormal cristae in skeletal muscle and heart tissues of KD-fed KO mice, respectively; bars, 10 μm; WT, n = 152; KO, n = 144 in (E) and n = 161; KO, n = 130 in (F).

(G) A treadmill test performed at the end of 10 weeks of KD feeding showed that the KD induced a higher number of falls in the KO mice during acute excise compared with the WT mice; n = 5 each.

(H) The fractional shortening (FS) rate in KO mice fed with KD for 10 weeks was significantly lower than that in KO-fed WT mice; n = 10–11.

(I) WT and KO mice at 8 weeks old were subject to TAC surgery. The KO mice showed a significant decrease in FS after TAC surgery.

(J) Cardiomyocytes were isolated from WT and KO mice 10 weeks after TAC. Calcium imaging revealed a decrease in the peak calcium influx in KO cardiomyocytes. The inserted graph shows the normalized peak amplitude of calcium influx in cardiomyocytes from WT and KO mice; n = 13 for WT and n = 6 for KO. Data are the mean ± SEM. *p < 0.05. **p < 0.01, ***p < 0.001, ****p < 0.0001.

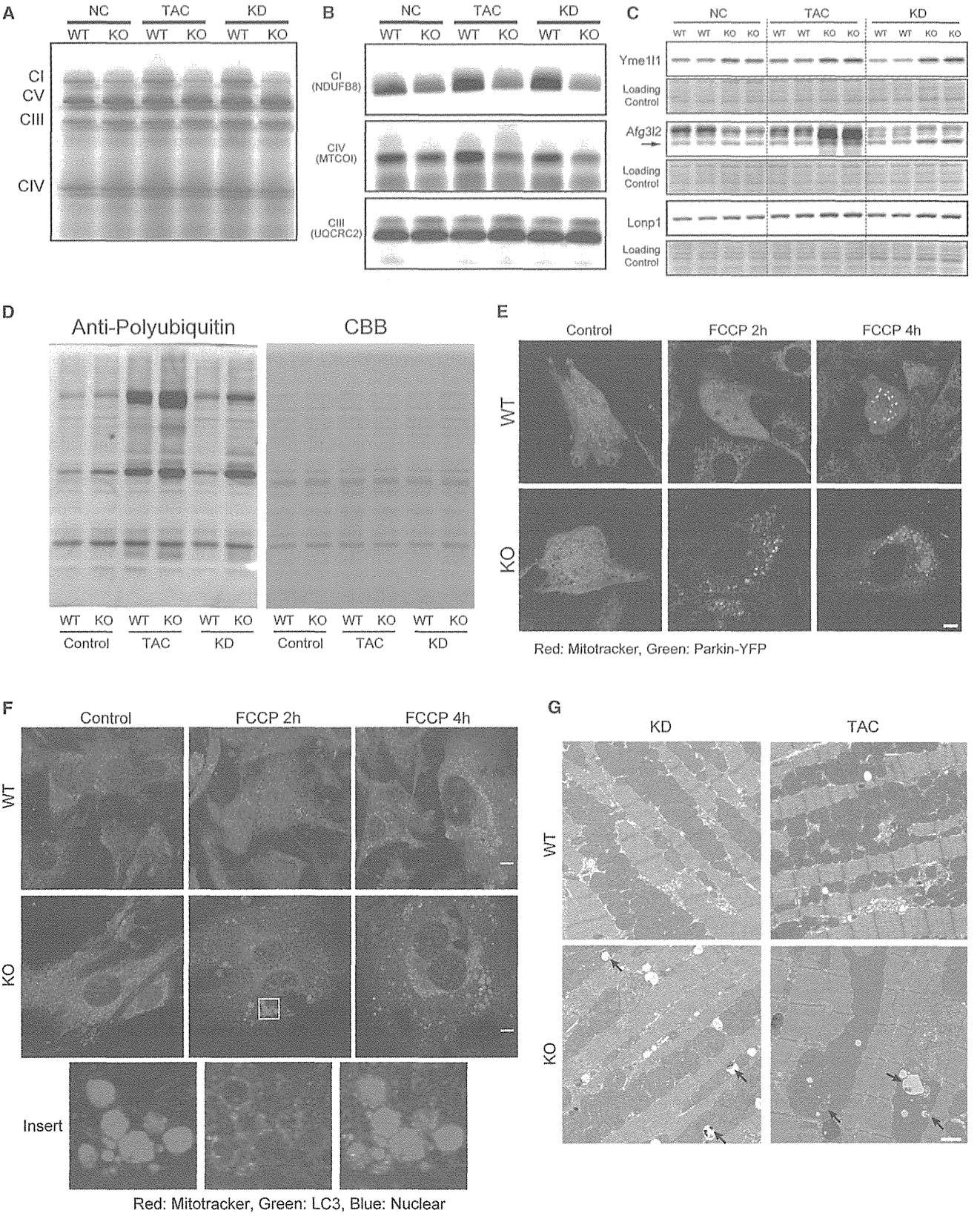

(legend on next page)

results demonstrate that stress-induced mitochondrial remodeling impaired mitochondrial protein synthesis and accelerated the decomposition of respiratory complexes, which triggered the mtUPR and mitophagy in KO mice. Thus, the accumulation of compromised mitochondria ultimately contributes to the development of myopathy and cardiac dysfunction.

Association of ms^2 Modification with Mitochondrial Disease

Because the pathological phenotypes of KO mice resembled those of mitochondrial disease, we speculated that ms^2 modification might be involved in mitochondrial disease. We investigated the ms^2 modification level in peripheral blood cells collected from MELAS patients who carry the A3243G mutation (Figure S7A). Because of the limited number of clinical RNA samples, we adapted the quantitative PCR-based method (Xie et al., 2013), which was originally developed to examine the ms^2 level of ms^2t^6A in cytosolic $tRNA^{Lys(UUU)}$, to sensitively examine the ms^2 modification level ms^2i^6A in mt-tRNAs (Figures S7B–S7E). Strikingly, the heteroplasmy level of mutant mt-DNA was significantly correlated with the ms^2 modification levels of four mt-tRNAs, but not with the cytosolic tRNALys(UUU) (Figures 7A–7D and S7F). Interestingly, the mutant mtDNA level was not correlated with the expression level of *CDK5RAP1*, suggesting that the decrease in ms^2 modifications was not due to a deficiency in Cdk5rap1 (Figures S5D–S5G). Because the A3243G mutation is located in the mtDNA region corresponding to mt-$tRNA^{Leu(UUR)}$, the decrease in the ms^2 levels of $tRNA^{Trp}$, $tRNA^{Phe}$, $tRNA^{Tyr}$, and $tRNA^{Ser(UCN)}$ was likely not caused by the A3243G mutation but, rather, was due to secondary effects. Cells bearing A3243G mutations in mtDNA exhibit a marked reduction of mitochondrial protein synthesis and an increase in the oxidative stress level (Crimi et al., 2005; Ishikawa et al., 2005). Because Cdk5rap1 contains highly oxidation-sensitive [4Fe-4S] clusters (Arragain et al., 2010), we speculated that the excess oxidative stress originated from mutant mitochondria might result in a collateral inhibition of Cdk5rap1 activity. Indeed, cells treated with sublethal doses of H_2O_2 showed a rapid decrease in ms^2 modification, which was completely reversed by adding 10 mM pyruvate, which serves as an antioxidant (Figures 7E–7G). In addition, treatment of cells with an NO donor such as SNAP and NOC18 significantly reduced the ms^2 modification level, which was reversed by the addition of the NO scavenger PTIO (Figure 7H). Taken together, these results suggest that oxidative stress-induced decreases in ms^2 modifications might compromise the quality of the mitochondria and contribute to the progression of mitochondrial disease.

DISCUSSION

Regulation of Mitochondrial Protein Synthesis by Cdk5rap1-Mediated ms^2 Modification

In the present study, we revealed the important physiological functions of ancient mitochondrial ms^2 modifications in mice and human. Using Cdk5rap1 KO mice, we provide direct evidence that Cdk5rap1 catalyzes the ms^2 modifications of mt-$tRNA^{Phe}$, mt-$tRNA^{Trp}$, mt-$tRNA^{Tyr}$, and mt-$tRNA^{Ser(UCN)}$ in mammalian cells. The ms^2 group at the A37 of tRNA can directly participate in crossstrand stacking with the first nucleotide of the codon of the mRNA to maintain the reading frame (Jenner et al., 2010). Indeed, a deficiency in the ms^2 modification of ms^2i^6A impaired reading frame maintenance in bacteria and caused defective mitochondrial protein synthesis in Cdk5rap1 KO mice. Interestingly, nuclear-encoded mitochondrial protein, such as NDUFB8 in complex I, was also decreased in KO mice. The indirect decrease of NDUFB8 is most likely due to the poorly assembled respiratory complexes in KO mice. A previous study has shown that a deficiency in a single subunit in complex I could compromise complex formation and cause the proteolysis of other subunits (Karamanlidis et al., 2013). Our results thus demonstrate that the ms^2 modification of mt-tRNAs is indispensable for mitochondrial protein synthesis and the proper assembly of respiratory complexes.

Whereas only one transcript of *Cdk5rap1* has been found in mice, multiple splicing variants of human *CDK5RAP1* are listed in the database (Figure S1A). One transcript of human *CDK5RAP1* encodes a short form of CDK5RAP1 without a mitochondrial localization signal (Q95SZ6-2 in Figure S1A), which raises the possibility that CDK5RAP1 might regulate cellular function by modifying cytosol RNAs (Reiter et al., 2012). However, there was no detectable ms^2i^6A in total RNA isolated from KO MEF cells expressing the cytosolic form of Cdk5rap1 with the enzyme activity preserved. These results clearly suggest that Cdk5rap1 does not modify nuclear DNA-derived RNAs in murine cells. Furthermore, the defective mitochondrial protein synthesis observed in Cdk5rap1 KO mice may be directly caused by the loss of ms^2 modifications in mt-tRNAs.

Deficiency of ms^2 Modification and Its Physiological Outcome

This study revealed unique phenotypic outcomes of Cdk5rap1 KO mice in response to distinct environmental conditions. Under sedentary conditions, the skeletal and cardiac functions of the

Figure 6. The Deficiency in ms^2 Modification Compromises Mitochondrial Protein Quality under Stressed Conditions

(A) Steady-state levels of CI, CIII, CIV, and CV in heart tissue in WT and KO mice treated with NC, KD, and TAC surgery were examined by BN-PAGE.

(B) The steady-state levels of CI protein NDUFB8, CIV protein MTCOI, and CIII protein UQCRC2 in heart tissue in WT and KO mice treated with NC, KD, and TAC surgery were examined by BN-PAGE followed by western blotting. UQCRC2 was used as a loading control.

(C) The protein levels of Yme1l1, Afg 3l2, and Lonp1 were examined in heart tissues from WT and KO mice treated with NC, KD, and TAC surgery. Membranes stained with CBB were used as a loading control.

(D) Enhanced polyubiquitination was observed in the mitochondria in the hearts of KO mice under each stress.

(E) WT and KO cells transfected with Parkin-YFP were treated with 10 μM FCCP for 2 and 4 hr; bar, 10 μm.

(F) WT and KO cells were treated with 10 μM FCCP for 2 and 4 hr. The cells were then stained with an anti-LC3 antibody and Mitotracker. The inserted box shows mitochondria surrounded by the LC3 protein and is magnified in the bottom panels; bar, 10 μm.

(G) Electron microscopy of mitochondria in heart tissue from WT and KO mice treated with KD or TAC surgery. Arrows indicate the autophagic vacuoles; bar, 10 μm.

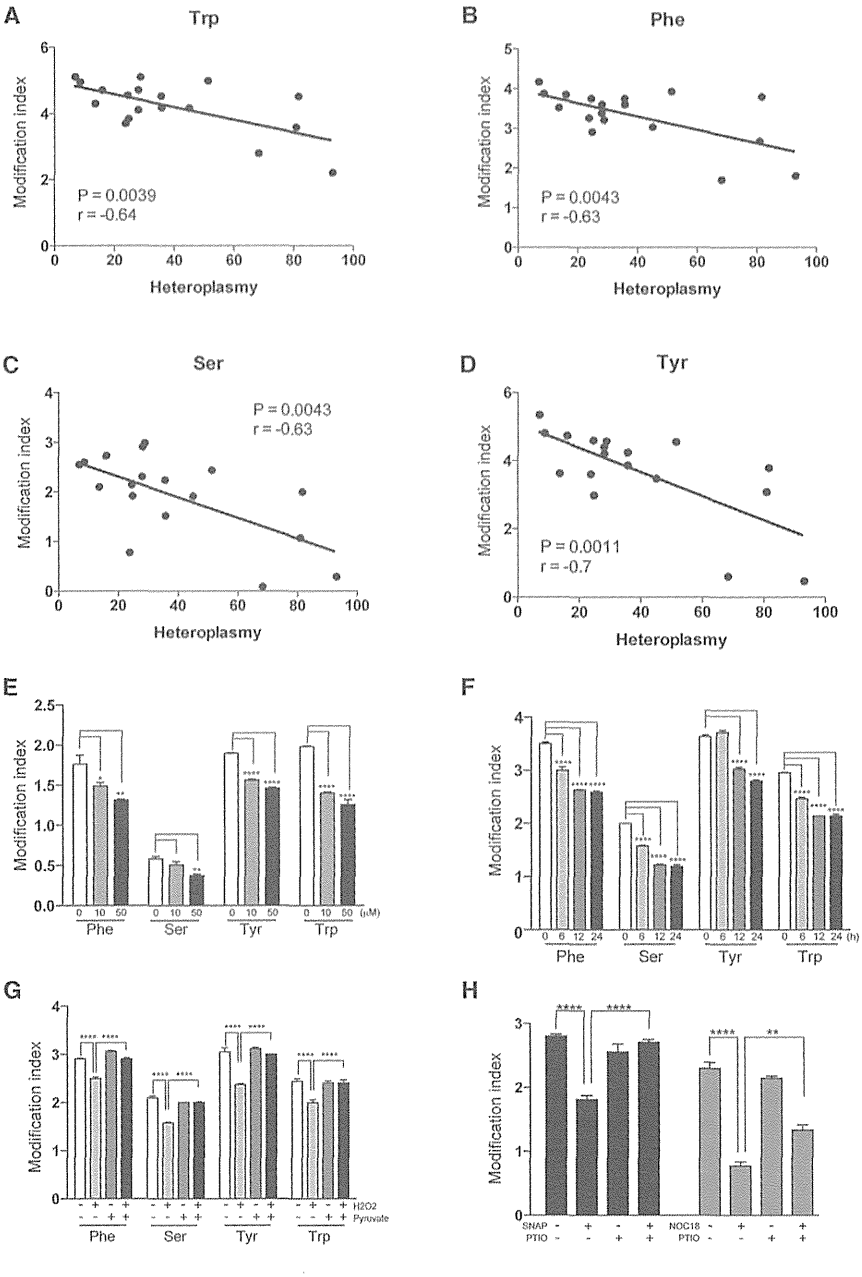

Figure 7. Association of ms^2 Modifications with MELAS

(A–D) Negative correlation of the ms^2 modification level of mt-tRNA^{Trp} (A), mt-tRNA^{Phe} (B), mt-tRNA$^{Ser(UCN)}$ (C), or mt-tRNA^{Tyr} (D) with the heteroplasmy level in MELAS patients; n = 18 each.

(E) Treatment with H_2O_2 reduced the level of ms^2 modification of mt-tRNAs in HeLa cells. Cells were treated with 10 μM or 50 μM H_2O_2 for 24 hr, and the ms^2 modification levels were examined by qPCR; n = 4 each.

(F) Time-dependent decreases in ms^2 modification after H_2O_2 treatment in HeLa cells. Cells were treated with 50 μM H_2O_2 for 6, 12, and 24 hr; n = 4 each.

(G) HeLa cells were treated with 50 μM H_2O_2 for 24 hr in the presence or absence of 10 mM pyruvate. The decrease in the ms^2 modification level was prevented by pyruvate; n = 4 each.

(H) HeLa cells were treated with NO donors, 100 μM SNAP or 100 μM NOC18 for 24 hr in the presence or absence of PTIO. The ms^2 modification level of mt-tRNA^{Trp} was examined by qPCR; n = 4 each. Data are the mean ± SEM. *p < 0.05. **p < 0.01, ****p < 0.0001.

Cdk5rap1 KO mice were compatible with those of the WT mice, despite the marked decrease in respiratory activities and regardless of the increase of oxidative stress. The mitochondrial dysfunction in KO mice might be compensated by the remodeling of mitonuclear protein balance, which serves as a protective mechanism by inducing mtUPR (Houtkooper et al., 2013). Indeed, in contrast to the decrease of mitochondrial protein synthesis, several cytosolic proteins appear to be upregulated in KO cells (right panels in Figure 2A). This mitonuclear protein imbalance might contribute to the upregulation of basal mtUPR in muscle and heart tissues of KO mice (Figure 6C). Furthermore, a collective increase of ROS metabolism genes, including ROS scavenger genes such as *ApoE*, *DHCR24*, and *SRXN1*, might ameliorate oxidative stress and protect the muscular and cardiac functions in KO mice. Similar to our results, previous studies have found no adverse phenotypes under basal conditions in transgenic mice with respiratory defects (Karamanlidis et al., 2013; Wenz et al., 2009). Our results thus support the current perspective that mitochondrial dysfunction, depending on its degree, may not immediately produce a pathological phenotype under sedentary conditions.

In contrast, under stressed conditions, Cdkrap1 KO mice exhibited apparent skeletal muscle and heart dysfunctions. The defective mitochondrial protein synthesis caused a marked decrease in protein levels and activities of complexes I and IV in KO mice under stressed conditions. The progressive disruption of respiratory complexes, which exaggerates mtUPR and mitophagy, thus largely compromised mitochondria quality and led to myopathy in KO mice. Recent studies have shown that Parkin-mediated mitophagy is critical for the removal of damaged mitochondria and thus protects cardiac function under stressed conditions (Hoshino et al., 2013; Chen and Dorn, 2013). However, given the observation of a number of degenerated mitochondria in KO mice (Figures 4D and 5G), the extent of mitochondria damage in KO mice was likely beyond the maintenance capacity of mitophagy, which ultimately led to catastrophic mitochondrial dysfunction and myopathy. In addition, the acceleration of complex I defect was associated with a modest increase of oxidative stress, which could trigger mtUPR and cause cytotoxicity in stressed KO mice (Runkel et al., 2013). However, compared with the progressive impairment of mitochondria quality, the degree of increase of ROS after mitochondrial stress was rather small in

stressed KO mice. Our results thus suggest that ROS might also contribute to the pathogenesis, but to a limited extent. The accumulation of malfunctioning mitochondria is likely the primary cause of the progression of myopathy in KO mice.

Regulation of ms^2 Modification by Oxidative Stress and Its Association with Human Disease

An important finding of this study is that the ms^2 modification levels were reduced in MELAS patients carrying the A3243G mutation in mt-$tRNA^{Leu}$. This result is surprising because mt-$tRNA^{Leu}$ does not contain an ms^2 modification. Previous studies have shown that the deficiency of taurine modification in mt-$tRNA^{Leu}$ carrying the A3243G mutation is the primary cause of MELAS (Kirino et al., 2005; Yasukawa et al., 2001). Given the significant association of the heteroplasmy level with the ms^2 modification level in MEALS patients, our results suggest that the myopathy in MELAS is caused not only by a decoding error at the Leu codon but also by decoding errors occurring at multiple codons, including Leu, Phe, Tyr, Trp, and Ser codons.

The reason A3243G in mt-$tRNA^{Leu}$ is associated with decreased modifications in other mt-tRNAs remains unclear. Although further studies are required to reveal the molecular mechanism, our results suggest that oxidative stress may be one of the reasons for this finding. Cdk5rap1 requires two [4Fe-4S] clusters for ms^2 group insertion (Forouhar et al., 2013); therefore, it is conceivable that ROS, such as H_2O_2 or $ONOO^-$, may oxidize these [4Fe-4S] clusters and inactivate Cdk5rap1. In support of our hypothesis, ROS-treated cells exhibited a rapid decrease in ms^2 modification that was effectively reversed by antioxidants. Thus, ROS generated by the mutation in mt-$tRNA^{Leu}$ might impair Cdk5RAP1-mediated ms^2 modification, which might further amplify mitochondrial dysfunction and ultimately accelerate myopathy in MELAS patients. In addition to mitochondrial disease, ms^2 modifications might be involved in a wide variety of human diseases in which ROS have been previously implicated, such as cardiac dysfunction and cancer (Schieber and Chandel, 2014).

In conclusion, this study reveals a unique quality control system in mitochondria by which the ms^2 modification of mt-tRNAs dynamically regulates mitochondrial protein synthesis and contributes to the development of myopathy in vivo. Our findings have important physiological implications for the basic mechanism of mitochondrial protein synthesis and provide insights into the pathological mechanism of mitochondrial disease.

EXPERIMENTAL PROCEDURES

Please see the Supplemental Experimental Procedures for additional details.

Animals

Cdk5rap1 KO mice were generated by crossing transgenic mice with exon 5 and 6 of *Cdk5rap1* floxed with LoxP sequence, with transgenic mice expressing Cre recombinase under the control of the CAG promoter. Mice were backcrossed to C57BL6/J mice for at least seven generations to eliminate Cre transgene and control genetic background. Littermates of WT and KO mice (8–12 weeks old) were used for experiments unless otherwise specified. Animals were housed at 25°C with 12 hr light and 12 hr dark cycles. A KD was purchased from Research Diets (D12369B). All animal procedures were approved by the Animal Ethics Committee of Kumamoto University (Approval ID, C25-163). Detailed information on genotyping can be found in the Supplemental Experimental Procedures.

Luciferase Assay

E. coli colonies were transformed with plasmids encoding dual *luciferase* for detecting decoding error, *GST-Cdk5rap1*, or dominant-negative *GST-Cdk5rap1*. Colonies were cultured at 37°C, and isopropyl β-D-1-thiogalactopyranoside (IPTG) was added to the cultures at a final concentration of 1 mM. After 1 hr of incubation, the cultures were harvested for the luciferase assay using the Dual-Luciferase Reporter Assay System (Promega). Detailed procedures for detecting decoding error can be found in the Supplemental Experimental Procedures.

Cell Culture and Transfection

Mammalian cells were grown in DMEM high-glucose medium (GIBCO) supplemented with 10% fetal bovine serum (FBS, HyClone) at 37°C and 5% CO_2. Transfection of the plasmid DNA was performed with Lipofectamine 2000 (Invitrogen).

Oxygen Consumption

The oxygen consumption rate in MEF cells and intact mitochondria was measured using an XF24 Analyzer (Seahorse Bioscience). The oxygen consumption rate was normalized to the total protein concentration for measurement in cells. Detailed procedures for the respiratory assay can be found in the Supplemental Experimental Procedures.

Gene Expression Assay

RNA was extracted from tissues using Trizol (Invitrogen) following the manufacturer's instructions. Quantitative PCR (qPCR) was performed using SYBR Premix Ex Taq (TAKARA). For examination of the expression levels of oxidative response genes, the results were normalized to the geometric mean of multiple reference genes (Hprt1, RPL13A, B2M, GAPDH, ACT). Then, a Z-transformation was applied to the results to calculate the *Z* score and construct a heatmap (Cheadle et al., 2003). The sequences of primers used can be found in the Supplemental Experimental Procedures.

Analysis of tRNA Modification

Total RNAs were isolated from bacteria and tissues using Trizol reagent (Invitrogen). RNA was digested with Nuclease P1 (Sigma) and subjected to mass spectrometry (Agilent 6460). For detecting tRNA modification using the qPCR-based method, we adapted a protocol described previously (Xie et al., 2013). Detailed procedures for the mass spectrometry and qPCR method can be found in the Supplemental Experimental Procedures. To measure the tRNA modification level in blood samples, blood samples were collected from MELAS patients using standard procedures approved by Kurume University (IRB#9715).

ATP Measurement

Small pieces of skeletal muscle and heart tissue were immediately dissected after sacrificing mice and snap frozen in liquid nitrogen until measurement. ATP was measured using the ATP Bioluminescence Assay Kit following the manufacturer's protocol (TA100, WAKO). The luminescence was measured using a Centro XS^3 LB960 (Berthold) and normalized to total protein concentration.

Cardiac Function Examination

Echocardiographs were examined in M-mode while the mice were under anesthesia using the Vevo2100 system (Fujifilm VisualSonics, Inc.) according to the manufacturer's instructions.

Statistical Analysis

Statistical analyses were performed using Prism 6 Software (GraphPad Software). An unpaired Student t test was used to test the differences between two groups. Analysis of variance (one-way ANOVA or two-way ANOVA) was used to test the difference among multiple groups followed by a post hoc examination of the p value between two groups. A two-tailed p value of 0.05 was considered statistically significant.